Andean Geology 53 (1): 49-79. January, 2026
doi: 10.5027/andgeoV53n1-3779

Andean Geology
www.andeangeology.cl

Litopterna (Mammalia) from the Santa Cruz Formation (Early-Middle Miocene), Río Chalía, Patagonia, Argentina

***E. Sebastián Monsalvo[1, 4], Gabriela I. Schmidt[1, 4], M. Susana Bargo[2, 3], Sergio F. Vizcaíno [2, 4]**

[1] *Laboratorio de Paleontología de Vertebrados, Centro de Investigación Científica y de Transferencia Tecnológica a la Producción (CICYTTP, CONICET-Gob. de ER-UADER), Materi 149, E3105BWA, Diamante, Entre Ríos, Argentina. sebawish3@gmail.com; gschmidt@cicyttp.org.ar*

[2] *División Paleontología Vertebrados, Facultad de Ciencias Naturales y Museo, Unidades de Investigación, Anexo Museo. Av. 60 y 122, B1900 La Plata, Argentina. msbargo@fcnym.unlp.edu.ar; vizcaino@fcnym.unlp.edu.ar*

[3] *Comisión de Investigaciones Científicas de la Provincia de Buenos Aires (CIC), Calle 526 e/ 10 y 11, 1900, La Plata, Buenos Aires, Argentina.*

[4] *Consejo Nacional de Investigaciones Científicas y Técnicas (CONICET), Godoy Cruz 2290, Buenos Aires, Argentina.*

** Corresponding author: sebawish3@gmail.com*

ABSTRACT. The southern margin of the Río Chalía valley (also known as Sehuen or Shehuen), Province of Santa Cruz, Argentina, offers excellent outcrops of the Early-Middle Miocene Santa Cruz Formation (SCF). However, the information about the faunal content of these levels is scarce due to insufficient prospection. This contribution reports Litopterna specimens collected in 2018 and 2019 from six localities on the southern margin of the Río Chalía valley, spanning a distance of ~30 km. Twenty-one specimens were collected, the majority belonging to Proterotheriidae (18), and three TO Macraucheniidae. These specimens include mandibular fragments, maxillae, and postcranial elements. Among Proterotheriidae, *Tetramerorhinus lucarius*, *Te. cingulatum*, *Thoatherium minusculum*, *Diadiaphorus majusculus*, *Anisolophus australis*, and *A. floweri* were identified, while the Macraucheniidae record corresponds to *Theosodon* sp. The taxa recorded in the Río Chalía area align with those recently reported for the SCF in other localities of the province, such as the Atlantic coast between Monte León and Río Gallegos, Río Santa Cruz, and Lago Posadas, as well as other sites across the extensive distribution of the SCF. These recent collections, with well-documented geographic and altitudinal reference, are valuable for verifying Ameghino's original descriptions and revisiting Santacrucian taxa.

Keywords: Systematics, Proterotheriidae, Macraucheniidae, Native Ungulates, Santacrucian.

RESUMEN. Litopterna (Mammalia) de la Formación Santa Cruz (Mioceno Temprano-Medio), Río Chalía, Patagonia Argentina. El margen sur del valle del río Chalía (Sehuen o Shehuen) (provincia de Santa Cruz, Argentina) ofrece excelentes afloramientos de la Formación Santa Cruz (FSC; Mioceno Temprano-Medio). Sin embargo, la información sobre el contenido faunístico de estos niveles es escasa debido a una prospección insuficiente. En este artículo se reportan ejemplares de Litopterna recolectados en 2018 y 2019 en seis localidades del margen sur del valle del río Chalía, a lo largo de ~30 km. Se identificaron 21 especímenes, la mayoría pertenecientes a Proterotheriidae (18), y tres a Macraucheniidae. Estos especímenes incluyen fragmentos mandibulares, maxilares y elementos postcraneales. Entre los Proterotheriidae, se identificaron *Tetramerorhinus lucarius*, *Te. cingulatum*, *Thoatherium minusculum*, *Diadiaphorus majusculus*, *Anisolophus australis* y *A. floweri*, mientras que el registro de Macraucheniidae corresponde a *Theosodon* sp. Los taxones registrados en el área de río Chalía concuerdan con aquellos reportados recientemente para la FSC en otras localidades de la provincia, como la costa atlántica entre Monte León y los ríos Gallegos, Santa Cruz y lago Posadas, así como otros sitios a lo largo de la extensa distribución de la FSC. Estas colecciones recientes, con procedencia geográfica y altitudinal bien documentada, son valiosas para verificar las descripciones originales de Ameghino y revisar los taxones santacrucenses.

Palabras clave: Sistemática, Proterotheriidae, Macraucheniidae, Ungulados Nativos, Santacrucense.

1. Introduction

South American native ungulates (SANUs) were a diverse group of herbivorous mammals that lived across South America for most of the Cenozoic. The main groups within SANUs: Astrapotheria, Pyrotheria, Xenungulata, Notoungulata, and Litopterna, flourished during this period of faunistic isolation (Patterson and Pascual, 1968; Simpson, 1980; Bond *et al*., 1995; Croft *et al*., 2020). While some SANUs occupied ecological roles comparable to those of modern hoofed mammals, others developed unique cranial and postcranial adaptations (Croft *et al*., 2020).

The proposed close relationship between SANUs and perissodactyls, grouped under Panperissodactyla, suggests that at least some SANUs belonged to Laurasiatheria, consistent with paleogeographic models (Croft *et al*., 2020). Collagen studies of *Toxodon* (Notoungulata) and *Macrauchenia* (Litopterna) identified them as sister taxa more closely related to perissodactyls than to other placental mammals (Buckley, 2015; Welker *et al*., 2015). Mitochondrial DNA from *Macrauchenia* supported this placement (Westbury *et al*., 2017).

A recent study tentatively divides the order Litopterna into two suborders: Eulitopterna and Notopterna. The first one includes the families Adianthidae, Macraucheniidae, Proterotheriidae, and Anisolambdidae (which encompasses Anisolambdinae and Sparnotheriodontinae), while Notopterna comprises Indaleciidae and Notonychopidae (Püschel *et al*., 2024).

Some authors have considered three subfamilies of Proterotheriidae: Anisolambdinae, Megadolodinae, and Proterotheriinae (Cifelli, 1983; Cifelli and Villarroel, 1997; Villafañe *et al*., 2006), while others included only the latter two following Soria's (2001) proposal to raise Anisolambdinae to family level within Litopterna (*e.g*., Corona *et al*., 2020; Schmidt *et al*., 2024), a taxonomic rank supported by the phylogenetic results of Püschel *et al*. (2024).

Proterotheriids were small to medium-sized cursorial ungulates, with some of them reaching the size of an antelope (Villafañe *et al*., 2006). They are recorded since the late Oligocene (excluding Anisolambdinae) and became extinct at the Late Pleistocene/Early Holocene boundary (Paula Couto, 1952; Pascual *et al*., 1996; Bond *et al.,* 2001; Vezzosi *et al*., 2009; Corona *et al*., 2018; Schmidt *et al*., 2019, 2024), being one of the most persistent groups within the South American Cenozoic record (Pascual *et al*., 1996; McKenna and Bell, 1997; Villafañe *et al*., 2006).

Macraucheniids were large animals with structurally robust mesaxonic and tridactyl limbs. They are recorded from the middle-late Eocene to the Early Holocene (Cifelli, 1983; Kerber *et al*., 2011; McGrath *et al*., 2020a) and declined after the Late Miocene, like Proterotheriidae. Ameghino (1902) included three subfamilies in Macraucheniidae: Macraucheniinae, Theosodontinae, and Cramaucheniinae, based on the position of the nasal opening relative to the premaxillaries and the development of the nasal bones. Posteriorly, Soria (1981) recognized only two: Cramaucheniinae and Macraucheniinae, including Theosodontinae within the former, as there are minimal differences between *Cramauchenia* and *Theosodon*, but substantial differences compared with later forms from Late Miocene and younger specimens. Some phylogenetic analyses using cladistic methods failed to support Cramaucheniinae as a distinct and monophyletic group (Schmidt and Ferrero, 2014; Forasiepi *et al*., 2016; McGrath *et al*., 2018; Püschel *et al*., 2023, 2024). However, Lobo *et al*. (2024) recovered two clades in their phylogenetic analysis of Macraucheniidae: Cramaucheniinae (including *Theosodon*) and Macraucheniinae (with *Llullataruca*).

Litopterns, notoungulates, and astrapotheres are well recorded in the Early-Middle Miocene Santa Cruz Formation (SCF) (Burdigalian-early Langhian) as part of the Santacrucian South American Land Mammal Age (SALMA) (Cassini *et al*., 2012). Litopterns are the second most abundant and diverse group in the SCF, only surpassed by Notoungulata (Pascual *et al*., 1996), with Proterotheriidae including as many as seven genera and 13 species (Soria, 2001; Villafañe *et al*., 2006; Ubilla *et al*., 2011), and Macraucheniidae represented only by the genus *Theosodon* with 10 species. Nevertheless, several of these species are based on fragmentary remains with questionable diagnoses, so the true number of species is likely lower (Scott, 1910; Soria, 2001; Croft *et al*., 2004; Cassini *et al*., 2012; Schmidt and Ferrero, 2014; McGrath *et al*., 2018).

The SCF is a continental fluvial succession widely distributed in Patagonia, with exposures along the Province of Santa Cruz, Argentina, and the Aysén and Magallanes regions in Chile (Fig. 1A), that preserves the best Neogene terrestrial records of southern South America, with abundant and diverse fossil vertebrates

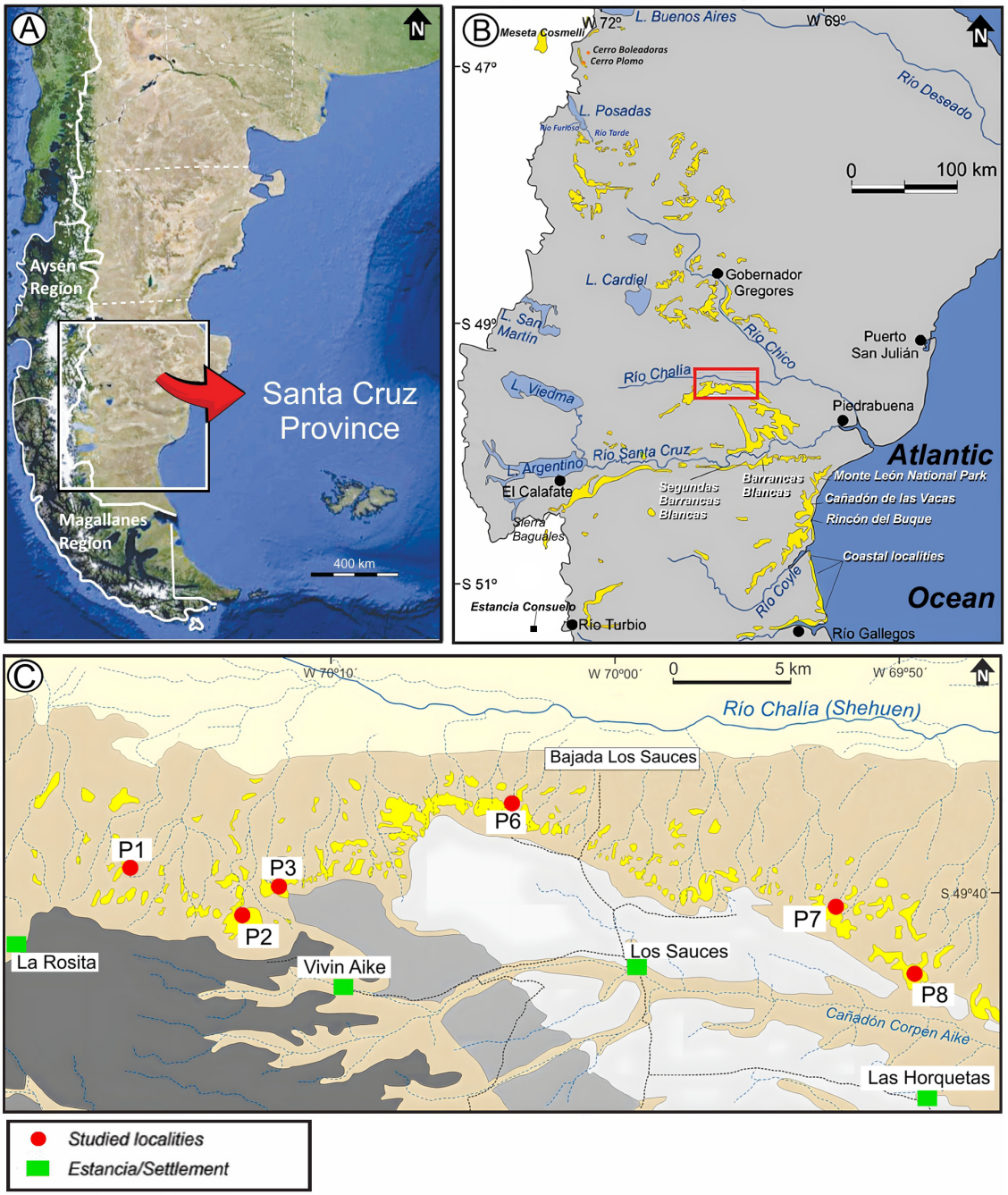

FIG. 1. **A.** Detail of Patagonia indicating the Santa Cruz Province. **B.** Map of southern Patagonia showing continental Miocene exposures (in yellow), mostly belonging to the SCF. Red rectangle indicates the study area. Black dots indicate localities. Text in italics refer to locations. **C.** Map of the study area showing the sampled localities (red dots) and settlements (green huts) visited during the field trips (2018-2019) (figure modified from Cuitiño *et al*., 2021).

that accumulated during the Middle Miocene Climatic Optimum (MMCO) (Trayler *et al*., 2020a; Cuitiño *et al*., 2021; Kay *et al*., 2012, 2021). The SCF outcrops are widespread: in the southeast, along the coastal region between the Monte León National Park and Río Gallegos (Vizcaíno *et al*., 2012a, b; Raigemborn *et al*., 2015, 2018; Trayler *et al*., 2020a, b); in the central region along the southern margins of the Río Santa Cruz (Fernicola *et al*., 2014, 2019; Cuitiño *et al*., 2016, 2019a; Kay *et al*., 2012, 2021) and the Río Chalía (Vizcaíno *et al*., 2018; Cuitiño *et al*., 2021) valleys; and in the northwest, in the surroundings of Lago Posadas (Cuitiño *et al*., 2019b) (Fig. 1B) and in Meseta Cosmelli (De la Cruz and Suárez, 2006). A Middle Miocene temporal overlapping of the SCF with the Collón Curá Formation, which bears a Friasian fauna (*sensu* Bondesio *et al*., 1980) in northern Patagonia has been recorded at the higher levels of Segundas Barrancas Blancas locality in the Río Santa Cruz (Cuitiño *et al*., 2016, 2019a) and P2-P3 localities at the Río Chalía (Cuitiño *et al*., 2021), and probably at Lago Posadas and Meseta Cosmelli (see Cuitiño *et al*., 2019b, and De La Cruz and Suárez, 2006). The SCF at the *Río* Chalía, provides a well-exposed fluvial succession that has yielded abundant and diverse fossil vertebrates deposited during the MMCO (Cuitiño *et al*., 2021).

Despite the SCF at the Río Chalía exposes some of the best outcrops in terms of lateral and vertical extension and span time, its paleontological content has so far been poorly studied in comparison with that of the Río Santa Cruz and the Atlantic coast localities (Vizcaíno *et al*., 2012b; Fernicola *et al*., 2019; Kay *et al*., 2012, 2021). In this contribution, we present and describe new remains of Litopterna (Proterotheriidae and Macraucheniidae) recently (2018-2019) recovered from the SCF along the Río Chalía valley (Fig. 1C), with accurate geographical and altitudinal information. This new collection will contribute to enhancing our understanding of the taxonomic richness of litopterns, allowing comparisons with other Santacrucian localities.

1.1. The record of litopterns in the Santa Cruz Formation

The specimens collected in 1887 by C. Ameghino in the SCF along the Río Santa Cruz allowed his brother F. Ameghino to name and describe the family Proterotheriidae and six species: *Proterotherium cavum*, *Thoatherium minusculum*, *Diadiaphorus velox*, *D. majusculus*, *Licaphrium floweri*, *L. parvulum*, and the macraucheniid *Theosodon lydekkeri* (Ameghino, 1887; Soria, 2001; Fernicola *et al*., 2019; Schmidt *et al*., 2019). Soria (2001) also assigned some specimens from the Río Santa Cruz to *Anisolophus australis* and *Tetramerorhinus mixtum.*

Schmidt *et al.* (2019) studied new Santacrucian litoptern remains (Proterotheriidae and Macraucheniidae) from the southern banks of the Río Santa Cruz. They recognized six species of Proterotheriidae (*Anisolophus australis*, *A. floweri*, *Tetramerorhinus lucarius*, *Te. cingulatum*, *Thoatherium minusculum*, and *Diadiaphorus majusculus*) and one Macraucheniidae (*Theosodon* sp.). Most of the litopterns recorded in this new collection were also identified in the Atlantic coast localities (Cassini *et al*., 2012; Fernicola *et al*., 2019), particularly within the coastal beds situated between the Río Coyle and the Río Gallegos. In this area, Tauber (1999) recognized five species of Proterotheriidae: "*Proterotherium*" *cavum* (=*Tetramerorhinus lucarius* after Soria, 2001), *Licaphrium floweri* (=*Anisolophus floweri* after Soria, 2001), *Diadiaphorus robustus* (=*D. majusculus* after Soria, 2001), *Thoatherium minusculum* and "*Proterotherium*" *intermedium* (=*Anisolophus australis* after Soria, 2001), and one Macraucheniidae, *Theosodon lallemanti*. Later, Cassini *et al.* (2012) performed the first paleobiological study of Santacrucian native ungulates recorded in the same coastal localities. The litopterns analyzed included five proterotheriids (*Anisolophus australis*, *Diadiaphorus majusculus*, *Tetramerorhinus cingulatum*, *Te. mixtum*, *Te. lucarius,* and *Thoatherium minusculum*) and the macraucheniids *Theosodon lydekkeri*, *The. gracilis*, *The. garretorum*, and *The. lallemanti*.

The first remains of Litopterna from the Río Chalía were recovered by C. Ameghino in his third field trip to Patagonia in 1890 and studied by F. Ameghino who identified as new species: *Proterotherium cingulatum*, *Thoatherium crepidatum* (Proterotheriidae), and *Theosodon fontanae* [sic] (Macraucheniidae) (Ameghino, 1891). Posteriorly, in his full revision of the family Proterotheriidae, Soria (2001) reassigned these species as: *Tetramerorhinus cingulatum* (*Proterotherium cingulatum*), *Thoatherium minusculum* (*Th. crepidatum*), and included several specimens from the *Río* Chalía in the species *Tetramerorhinus mixtum*, *Anisolophus floweri*, *A. minusculum*, and "*Licaphrium*" *debile* (*nomen dubium*) (Soria, 2001).

In the northwest area of the Province of Santa Cruz, close to the Andes, the SCF exposures at Lago Posadas have yielded several fossil vertebrates, including litopterns collected during pioneering expeditions from Princeton University led by J.B. Hatcher in 1898-1899. These collections were described by Scott (1910) and are currently housed at the Yale Peabody Museum (New Haven, USA). Hatcher referred to this area around Lago Posadas, between the Río Furioso to the west and the Río Tarde to the east, as "Lake Pueyrredon". Additional specimens from Lago Posadas were obtained during recent expeditions led by S.F. Vizcaíno in 2016. The taxa recorded for this area include the proterotheriids *Tetramerorhinus lucarius*, cf. *Diadiaphorus*, *Licaphrium pyneanum* (=*Anisolophus floweri*), *Proterotherium dodgei* (=*Te. mixtum*), the macraucheniid *Theosodon gracilis*?, and Litopterna indet. (Cuitiño *et al*., 2019b).

It is interesting to mention that north of Lago Posadas, in the western slope of the Meseta of Lago Buenos Aires, the Early-Middle Miocene continental Cerro Boleadoras Formation (CBF) crops out in the Cerro Boleadoras and the Cerro Plomo localities (see Fig. 1B). This formation temporally overlaps with the middle and upper sections of the SCF in the Austral-Magallanes Basin of southern Patagonia. Vizcaíno *et al*. (2022) reported a new collection of fossil vertebrates from the CBF, recovered in 2020, which are typically Santacrucian in age. Two proterotheriids were reported from this area: *Thoatherium minusculum* and *Anisolophus* sp. On the other hand, Kramarz and Bond (2005) recorded the proterotheriids *Tetramerorhinus cingulatum* and *Diadiaphorus*? *caniadensis*, and the macraucheniid *Theosodon* (*Theosodon* sp.) from the upper levels of the Pinturas Formation, that might correlate with the lowest section of the SCF (Fleagle *et al*., 2012).

Records of Proterotheriidae and Macraucheniidae have been also documented in the SCF in Chile. Marshall and Salinas (1990) reported *Theosodon lallemanti* from Estancia Consuelo, near Puerto Prat in the Magallanes Region, and Croft *et al*. (2004) recorded an unidentified species of *Theosodon* in the Santacrucian Chucal fauna of northern Chile. In the Sierra Baguales area (Magallanes Region), fossiliferous outcrops of the SCF yielded *Paramacrauchenia scamnata* along with an additional yet unidentified proterotheriid (Bostelmann *et al*., 2013). At Meseta Cosmelli, also known as Meseta Guadal (Aysén Region), Buldrini (2017) and Buldrini and Bostelmann (2017) reported indeterminate proterotheriid remains from the SCF. Finally, McGrath *et al*. (2020a) described litopterns from the nearby Pampa Castillo local fauna, identifying two proterotheriids (*Thoatherium* and *Picturotherium*) and one macraucheniid (*Theosodon*). Based on these taxa, McGrath *et al.* (2020a) supported a Santacrucian age for the Pampa Castillo fauna, and suggested a biochronological correlation with the lower and middle levels of the Pinturas Formation.

2. Geological setting of the Santa Cruz Formation at the Río Chalía

The SCF was deposited during the Early-Middle Miocene (Burdigalian-early Langhian) by a floodplain-dominated fluvial system that drained the Patagonian Andes in the west to the Atlantic Ocean in the east under the influence of intense pyroclastic input. It is mainly composed of mudstones, tuffaceous sandstones and tuffs (Matheos and Raigemborn, 2012; Cuitiño *et al*., 2016, 2019a, b, 2021). At the Río Chalía, the SCF is exposed over a distance exceeding 30 km along the southern margin of the valley, and its thickness increases gradually from east to west, reaching up to 300 m (Cuitiño *et al*., 2021). It lies conformably over the marine Monte León Formation and the radiometric ages obtained by Cuitiño *et al*. (2021) indicate that the SCF accumulated between ~18 to 15.2 Ma. The uppermost boundary was recorded at the P3 locality. The correlation of the outcrops of different Miocene formations along the Santa Cruz Province is summarized in Vizcaíno *et al*. (2022).

3. Materials and methods

The new remains reported in this contribution come from the southern escarpment of the Río Chalía valley (Fig. 1C), west from where the river joins the Río Chico, in the Corpen Aike Department (Cuitiño *et al*., 2021). Two intensive fieldworks were carried out in 2018 and 2019 by joint expeditions of the Museo de La Plata and Duke University (North Carolina, USA). Six fossiliferous localities were surveyed along ~30 km, named from west to east: P1 Estancia La Rosita; P2 and P3 Estancia Vivin Aike; P6 Estancia Los Sauces; and P7 and P8 Estancia Las Horquetas (Fig. 1C). The fossil vertebrate collection was affected by the height and slope of the outcrops.

Since the majority of the collection were composites of loose specimens, assigning fossils to specific facies was difficult. Moreover, as no regional marker beds were recognized in the area, elevation was used as the best reference for correlating strata laterally. Three altitudinal (not strictly stratigraphic) ranges/levels in each locality were distinguished: A (150-250 m a.s.l.), B (250-350 m a.s.l.), and C (350-400 m a.s.l.), and all the specimens collected referred to any of these levels. Geographic coordinates of the collection sites were obtained using conventional GPS tools.

Twenty-one specimens of litopterns (18 Proterotheriidae and three Macraucheniidae) were collected (see Appendix for a full description). They were deposited in the Museo Regional Provincial Padre Manuel Jesús Molina, Río Gallegos, Santa Cruz Province, Argentina. Most remains correspond to dental and cranial elements. Every identifiable specimen was described, photographed, and measured with a caliper, registering its measurements in millimeters. The taxonomic assignments were carried out by morphological and metrical comparisons using bibliographic data. The dental terminology followed Soria (2001), Kramarz and Bond (2005), Bärmann and Rössner (2011), Villafañe *et al.* (2012), Schmidt (2015), and McGrath *et al*. (2020b) (Fig. 2), while the postcranial descriptions followed Scott (1910), Soria (2001), Ginot *et al*. (2016), Bai *et al*. (2017), and Harbers *et al*. (2020).

The specimens studied are housed in the following institutions: **AMNH**, American Museum of Natural History, New York, USA; **FMNH**, The Field Museum, Paleontology Collection, Chicago, USA; **MACN-A** and **MACN-PV**, Ameghino and Vertebrate Paleontology collections, respectively, Museo Argentino de Ciencias Naturales Bernardino Rivadavia, Buenos Aires, Argentina; **MLP-PV**, Vertebrate Paleontology Division, Museo de La Plata, La Plata, Argentina; **MPEF-PV**, Paleovertebrate Collection, Museo Paleontológico Egidio Feruglio, Trelew, Argentina; **MPM-PV**, Vertebrate Paleontology Division, Museo Regional Provincial Padre Manuel Jesús Molina, Río Gallegos, Argentina; **UATF-V**, Vertebrate Paleontology Collections, Universidad Autónoma Tomas Frías, Potosí, Bolivia; **YPM-VPPU**, Yale Peabody Museum, Vertebrate Paleontology Princeton, University Collection, New Haven, USA.

Anatomical and metrical abbreviations, **buc:** buccal cingulum, **cfo:** central fossette, **copr:** coracoid process, **csul:** calcaneal sulcus, **cubf:** cuboid facet, **D/d:** deciduous, **dfo:** distal fossette, **dlg:** distolingual groove, **ecf:** ectal facet, **efl:** entoflexid, **end:** entoconid, **enld:** entolophid, **es:** entostyle, **fibf:** fibular facet, **fo:** frontal foramina, **hyld:** hypoconulid, **hys:** hypostyle, **L:** length, **M/m:** upper/lower molar, **med:** metaconid, **mef:** median fossette, **mfl:** metaflexid, **mfo**: metacone fold, **mlc:** mesiolingual cingulum/cingulid, **mt:** metastyle, **mtl:** metaconule, **mx:** maxilla, **na:** nasal, **P/p:** upper/lower premolar, **pad:** paraconid, **par:** paralophid, **pcr:** postcristid, **pfo:** paracone fold, **phyc:** prehypocrista, **ps:** parastyle, **psd:** parastylid, **psmcd:** postmetacristid, **supf:** supplementary facet for the astragalus, **sus:** sustentaculum, **susf:** sustentacular facet, **tli:** third lobe inflection, **W:** width.

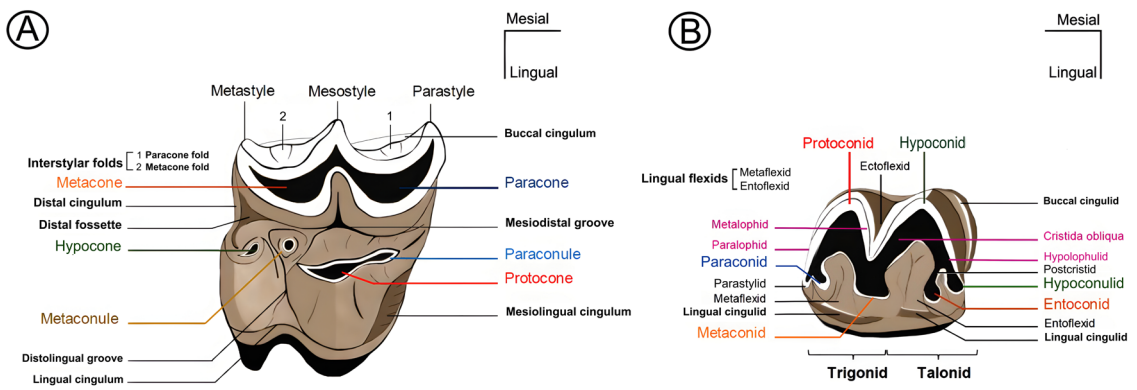

FIG. 2. Schematic drawings and dental nomenclature of proterotheriid molars in occlusal view. A, upper; B, lower (modified from Schmidt, 2015). Main cusps are indicated by distinct colors. In B, lophids are highlighted in violet.

4. Results

Systematic paleontology

No rank Panperissodactlya Welker *et al*., 2015
Order Litopterna Ameghino, 1889
Family Proterotheriidae Ameghino, 1887
Subfamily Proterotheriinae Ameghino, 1887
Genus ***Tetramerorhinus*** Ameghino, 1894

Type species: *Tetramerorhinus fortis* Ameghino, 1894. Santa Cruz Formation (Early-Middle Miocene), Monte Observación, Province of Santa Cruz, Argentina.
Referred species: *Te. lucarius* Ameghino, 1894, *Te. cingulatum* (Ameghino, 1891), *Te. mixtum* (Ameghino, 1894), *Te. prosistens* (Ameghino, 1899), and *Te. fleaglei* (Soria, 2001).

Tetramerorhinus lucarius Ameghino, 1894
(Fig. 3A-E; Tables 1 and 2)

List of synonymies: See Soria (2001, p. 42).
Holotype: MACN-A 3021; rostral portion of the skull with right P1-M2 and left P1-2, P4-M3.
Referred material: MPM-PV 21907; right premaxillary fragment with a small incisor, left maxillary fragment with DP3-4, right mandibular fragment with dp1-4, and left mandibular fragment with broken dp4 and m1 in the alveolar cavity.
Geographic provenance: Río Chalía, P2 locality.
Stratigraphic provenance: Santa Cruz Formation (Early-Middle Miocene, Santacrucian SALMA).
Description: MPM-PV 21907 consists of various fragments belonging to the same individual. Laterally, the premaxillary fragment (Fig. 3A) is triangular in shape, buccally convex, and lingually concave. The dorsal border is rounded and wide while the ventral is narrow. The incisor is small and conical, with its tip broken. The anterior border follows the dorsal curvature of the premaxilla, while the posterior one forms an obtuse angle with the ventral border. A tiny central channel can be observed through the broken end of the tooth. The DP3 and DP4 (Fig. 3B) are unworn, although DP3 has a more worn protocone and hypocone. DP3 is longer than wide. The lingual cusps are lower than the buccal ones. The paracone is slightly smaller than the metacone. The hypocone is larger than the protocone and slightly buccally placed, with its rounded base extending quite lingually, making the distal wall of the tooth wider than the mesial one. The paraconule is narrow and connects to the protocone through an oblique enamel ridge, which continues in an obtuse angle up to the paracone. Protocone and hypocone are joined by an enamel ridge that contains an entostyle at its base (Bärmann and Rössner, 2011) (Fig. 3B). The metaconule is absent. The mesostyle is more developed than the parastyle and the metastyle. In DP3 and DP4, a conspicuous buccal cingulum is present, and the buccal folds of the paracone and the metacone are well developed in DP3. The DP4 is wider and more quadrangular than the DP3. The protocone is larger than the hypocone. The paraconule and the mesiolingual cingulum are more developed than in DP3. A small metaconule is close to the protocone and interrupts the distolingual groove (Fig. 3B). The buccal styles are well developed, with the mesostyle being the most prominent. The buccal concavities are deeper than in DP3, and only the paracone fold is present.

The right mandibular ramus of MPM-PV 21907 (Fig. 3C, D) is low and thin. The dp1 is very small and compressed, with a triangular and slightly convex buccal wall. In occlusal view, it has a single central cusp (or protoconid) where the tooth thickens. The buccal cingulum is absent and the lingual is poorly developed. The dp2 is also triangular in buccal view, but larger than dp1. The paralophid curves anteriorly and bifurcates mesially into a poorly developed parastylid and a paraconid. The ectoflexid is shallow. The buccal and lingual cingula are weak. The dp3 is larger than the previous teeth and molarized. The trigonid and the talonid are similar in length, but latter is wider. The paralophid curves ending in a well-developed paraconid and a small parastylid. The metaconid is also well-developed and mesiodistally symmetrical. The hypolophulid ends with a hypoconulid, and the entoconid is differentiated. The dp4 has a trigonid longer and narrower than the talonid. The paralophid curves lingually and ends in a rounded paraconid (Fig. 3D). The metaconid is larger and taller than in the previous teeth. At the end of the hypolophulid, there is a small hypoconulid better developed than in dp3, and a tiny entoconid attached to it in a mesiolingual position (Fig. 3D). The talonid of the m1 presents a well-differentiated entoconid and hypoconulid (Fig. 3E).
Comments: Among the Santacrucian proterotheriids, the presence of a bunoid metaconule near the protocone in DP4 is an exclusive feature of the upper molars of *Tetramerorhinus*. The small size and general morphology of DP3-4 in MPM-PV 21907 are similar to those of *Te. lucarius* (MACN-A 190;

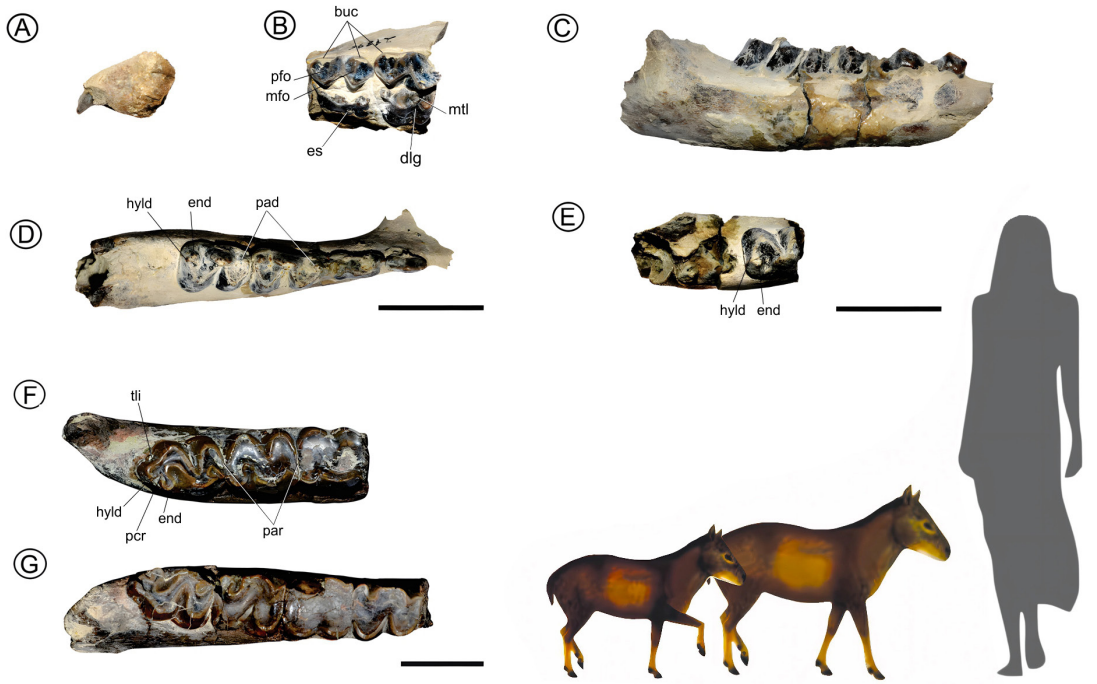

FIG. 3. **A-E.** ***Tetramerorhinus lucarius*****,** MPM-PV 21907. **A.** Right premaxillary fragment with a small incisor (lateral view). **B.** Left maxillary fragment with DP3-4 (occlusal view). **C-D.** Right mandibular fragment with dp1-4 (buccal and occlusal views). **E.** Left mandibular fragment with broken dp4 and m1 in the alveolar cavity (occlusal view). **F-G.** ***Tetramerorhinus cingulatum*****,** MPM-PV 21874. Left and right mandibular fragments with m1-m3 and p4-m3, respectively (occlusal views). Scale bars: 20 mm. Silhouettes of proterotheriids modified from Cassini *et al*. (2012).

TABLE 1. UPPER TOOTH DIMENSIONS OF THE STUDIED LITOPTERN SPECIMENS.*

Specimen No.	Taxon name		DP2	DP3	DP4	P2	P3	P4	M1	M2	M3
MPM-PV 21907	*Tetramerorhinus lucarius*	L		11.1/-	11.7/-						
		W		10.5/-	12.5/-						
MPM-PV 21877	*Thoatherium minusculum*	L	10.9/-	10.2/-	10.5/-				13.5/-		
		W	6.6/-	10.3/-	12.2/-				15.1/-		
MPM-PV 21899	*Thoatherium minusculum*	L							-/12.1	13.1/?	13.7/13.6
		W							-		-
MPM-PV 21881	*Diadiaphorus majusculus*	L					-	-/17.5			
		W					-	-			
MPM-PV 21882	*Diadiaphorus majusculus*	L					15.1/-		-/20.1	21/-	-/16.6
		W					-		-	-	-/20.6
MPM-PV 21884	*Diadiaphorus majusculus*	L				-	15.9/-				
		W				-	-				
MPM-PV 21880	*Anisolophus floweri*	L								14.6/-	
		W								-	
MPM-PV 21876	*Theosodon* sp.	L					17.3/-				
		W					15.1/-				

* Left/Right; -: missing data; ?: not measurable. Measurements in mm.

TABLE 2. LOWER TOOTH DIMENSIONS OF THE STUDIED LITOPTERN SPECIMENS.*

Specimen No.	Taxon name		dp1	dp2	dp3	dp4	p2	p3	p4	m1	m2	m3
MPM-PV 21907	*Tetramerorhinus lucarius*	L	-/11.8	-/10.6	-/12.1	-/11.3						
		W	-/3.5	-/4.3	-/7.4	8.6/8.7						
MPM-PV 21874	*Tetramerorhinus cingulatum*	L							-/14.2	14.8/15	15.5/15.3	17.6/17.5
		W							-/12.1	13/13.1		12.2/12.6
MPM-PV 21903	*Thoatherium minusculum*	L		-/9.5								
		W		-/4.1								
MPM-PV 21899	*Thoatherium minusculum*	L									13.1/-	13,5/13.5
		W									8.8/-	8.5 /8.3
MPM-PV 21900	*Thoatherium minusculum*	L			-	12.1/-						
		W			6.5/-	7.9/-						
MPM-PV 21937	*Thoatherium minusculum*	L						12.5/-	- /15.1	13.6/15.1	15.5/16.4	14.8/15.1
		W						7.5/-	9.1/10.1	9.6/11.2	9.1/10.3	7.7/8.6
MPM-PV 21902	*Diadiaphorus majusculus*	L						-	18.2/-			
		W						-	12.9/-			
MPM-PV 22340	*Diadiaphorus majusculus*	L										-
		W										-/11,5
MPM-PV 21898	*Anisolophus australis*	L							11.2/-			
		W							9.3/-			
MPM-PV 21878	*Anisolophus australis*	L					10.4/-		11.1/-	11.5/-		12.1/-
		W					5.7/-		9.4/-	/-		-
MPM-PV 21879	*Anisolophus australis*	L							-	-/10.8	-/12.8	-
		W							-	-/10.9	-/10.1	-/7.1
MPM-PV 21905	*Anisolophus floweri*	L									-/15.3	
		W									-/12.5	
MPM-PV 21901	*Anisolophus floweri*	L										-/18.7
		W										-
MPM-PV 21883	*Theosodon* sp.	L			21.4/-							
		W			10.6/-							

* Left/Right; -: missing data; ?: not measurable. Measurements in mm.

Soria, 2001). The absence of this feature in DP3 is also observed in MACN-A 11625 of *Te. prosistens*. However, we were unable to verify this in the remaining species of *Tetramerorhinus* (*Te. fleaglei*, *Te. cingulatum*, and *Te. mixtum*) due to the scarcity of deciduous remains.

Regarding the lower dentition, the small size and the presence of a small entoconid in dp4-m1 in MPM-PV 21907 are shared features with *T. lucarius* (MACN-A 1843-44 and MACN-A 3020; Soria, 2001). We exclude the assignment to *Thoatherium minusculum* (which is comparable in size) because it lacks the entoconid throughout the dental series, including the deciduous teeth (MPM-PV 4292, 3486, 19459). MPM-PV 21907 differs from the species of *Anisolophus* in terms of hypsodont teeth, a thinner enamel layer, excavated flexids, a well-developed paralophid and paraconid, and a smaller entoconid.

Tetramerorhinus cingulatum (Ameghino, 1891)
(Fig. 3F, G; Table 2)

List of synonymies: See Soria (2001, p. 51).
Holotype: MACN-A 3065-66; right hemimandible with p4-m3 and left one with m2-3.
Referred material: MPM-PV 21874; right mandibular ramus with p4-m3 and left mandibular ramus with m1-m3.
Geographic provenance: Río Chalía, P7 locality.
Stratigraphic provenance: Santa Cruz Formation (Early-Middle Miocene, Santacrucian SALMA).
Description: MPM-PV 21874 is heavily worn, which indicates that corresponds to an adult specimen. In all teeth, the metaconid is mesiodistally elongated and the highest cusp and both buccal and lingual cingulids are poorly developed. On the buccal side of the right hemimandible, a small mental foramen is located near the ventral border between p4-m1. This border exhibits a very smooth curve.

In occlusal view, the trigonid of p4 is shorter, narrower, and taller than the talonid. The paralophid nearly reaches the lingual side, but is shorter than the hypolophulid, resulting in the hypoconulid being more lingually positioned than the paraconid (Fig. 3G). The protoconid is more rounded than the hypoconid, and both cusps are separated by a wide and shallow ectoflexid. A large contact surface is observed between the hypolophulid of p4 and the paralophid of m1. The entoflexid is deeper than the metaflexid. The m1 is almost symmetrical and the trigonid of exhibits a wide concavity due to wear. The protoconid and the hypoconid are similar in size and buccally rounded. Small denticles can be observed at the base of the protoconid and near the poorly developed ectoflexid. The paralophid extends to the lingual side, and the paraconid is separated from a large metaconid by a small metaflexid (Fig. 3F, G). The lingual side of the talonid is broken. In m2 the trigonid is shorter than the talonid. The protoconid is more rounded and buccally positioned than the hypoconid, similar to m3. The paraconid is separated from the metaconid by a small notch. Buccally, the cingulid surrounding the protoconid presents small denticles. The ectoflexid is deep and wide. The left m2 presents a well-developed entoconid and a tiny hypoconulid, but in the right m2 both cusps are indistinguishable. The entoflexid extends deeper than in the previous teeth describing a fin shark shape. The metaconid is mesiodistally elongated. The m3 is asymmetrical, with the talonid longer than the trigonid. The lingual contour is convex following the curvature of the jaw, contrasting with the straight lingual border observed in p4-m2. The cingulid bordering the protoconid displays small denticles near the ectoflexid. The ectoflexid is deep and wide. The paralophid is shorter than in m1-2 and finishes in an acute paraconid. The metaconid projects forward towards the paraconid, enclosing the small metaflexid and forming a tiny enamel lagoon. The cristida obliqua is narrow and obliquely directed to the metaconid. A large hypoconulid is located distolingually after a buccal fold of the hypolophulid which is also marked by an external inflection, creating a well-developed third lobe (Fig. 3F, G). The entoconid is larger than the hypoconulid, more lingually placed, and is connected by a postcristid partly with the buccal portion of the hypoconulid and partly with the hypolophulid. The entoflexid is well-developed.

Comments: The presence of a long paralophid with paraconid in m2-3 and a third lobe in m3 allows us to assign MPM-PV 21874 to the genus *Tetramerorhinus*. The size and morphology of the teeth are comparable to specimens of *Te. cingulatum*, such as MACN-A 3065-66 (holotype), MACN-A 8665 (type of the synonym; Soria, 2001), and MACN-A 3062 (specimen referred by Soria, 2001).

Genus ***Thoatherium*** Ameghino, 1887

Type species: *Thoatherium minusculum* Ameghino, 1887. Santa Cruz Formation (Early-Middle Miocene), Río Santa Cruz, Province of Santa Cruz, Argentina.

Thoatherium minusculum Ameghino, 1887
(Fig. 4A-R; Tables 1 and 2)

List of synonymies: See Soria (2001, p. 57-58).
Holotype: Mandibular fragment with symphysis and part of the dentition (*fide* Ameghino, 1889). Not found. Belongs to the MLP-PV.
Referred material: MPM-PV 21877; left maxillary fragment with roots of DP1-4 and M1. MPM-PV 21903; right dp2. MPM-PV 21899; isolated teeth; right: M1, M3, p4, m3; left: M1-M3, m2-3. MPM-PV 21900; incomplete left dp3 and dp4. MPM-PV 21937; skull portion associated with a left mandibular fragment with p3-m3 and a right one with p4-m3.
Geographic provenance: Río Chalía. MPM-PV 21877 comes from P2 locality; MPM-PV 21903 comes from P8 locality; MPM-PV 21899 and MPM-PV 21900 come from P2 and P3 localities, respectively; and MPM-PV 21937 comes from P6 locality
Stratigraphic provenance: Santa Cruz Formation (Early-Middle Miocene, Santacrucian SALMA).
Description: The skull fragment MPM-PV 21937 (Fig. 4A) consists of the anterior portion of the frontal bones, with both orbits partially preserved, as well as the posterior section of the nasal and maxillary bones. On each frontal bone, there are two frontal foramina and two frontal grooves (Fig. 4A). As a result of shear distortion, the left foramen and the orbit are more anteriorly placed compared to the corresponding structures on the right side. In lateral view, the edge of both orbits is slightly arched and exhibits small roughness.

In MPM-PV 21877 (Fig. 4B; Table 1), DP1-4 only preserve the roots. The M1 is unworn, the buccal cusps are higher than the lingual ones and separated by a deep mesiodistal groove. The parastyle and the mesostyle are well developed and point outward, while the metastyle is less developed and points distally. The interstylar folds are faint, but the paracone fold is more pronounced than the metacone fold. The paracone is smaller than the metacone. Paraconule, protocone, and hypocone are laterally joined. The protocone is the most developed. A lophoid metaconule extends buccally and distally from the contact between the protocone and hypocone to join the metacone (Fig. 4B). The distolingual groove is shallow. The mesiolingual cingulum is represented as a low oblique ridge that is not fused with the base of the protocone, creating an open groove lingually (similar to *Paramacrauchenia* molars). There is no lingual cingulum between protocone and hypocone.

In MPM-PV 21899 (Fig. 4C), the right M1 lacks its buccal side. Paraconule, protocone, and hypocone are similar in size and are connected laterally due to wear. The mesiolingual cingulum projects from the anterior half of the paraconule up to the base of the protocone. A deep mesiodistal groove is bordered mesially by the paracone and the paraconule and distally by the lophoid metaconule, which extends somewhat obliquely from the posterior half of the metacone towards the anterior portion of the hypocone. This septum defines an oval-shaped distal fossette (Fig. 4C). The left M1 is identical to the right one, but more deteriorated (Fig. 4D). The left M2 (Fig. 4E) is also buccally broken, slightly larger, and less worn than M1 (Table 1). The lingual side of the paracone is more acute than the metacone and the paraconule is barely worn. The lophoid metaconule projects transversally from the metacone to the septum formed by the confluence of protocone and metacone. The protocone is smaller than the hypocone which is unworn. The distolingual groove is slightly marked. The mesiolingual cingulum projects from the mesial end of the paraconule to the base of the protocone, firstly concave and then convex. The central fossette is wide almost forming a mesiodistal groove. The metaconule does not completely define a distal fossette (Fig. 4E). Finally, both M3 (Fig. 4F, G) lack their buccal side; only the lingual portions of the paracone and metacone are preserved, both positioned obliquely relative to the mesiodistal axis. The paraconule joins the protocone obliquely and both are well developed. The hypocone is small and divided by a groove. There is no metaconule. The mesiodistal groove is deep and the mesiolingual cingulum is narrow and undulated.

Regarding lower teeth, the dp2 of MPM-PV 21903 (Fig. 4H, J; Table 2) is elongated, laterally compressed, triangular in lateral view, and oval in cross-section. The protoconid is high and well-developed. The ectoflexid is poorly developed. The paralophid splits into a weak lingual paraconid and a more mesobuccal parastylid (Fig. 4H, J). The metaconid is distolingually oriented and the metalophid is short and arched. Both the buccal and lingual cingulids exhibit weak crenulations.

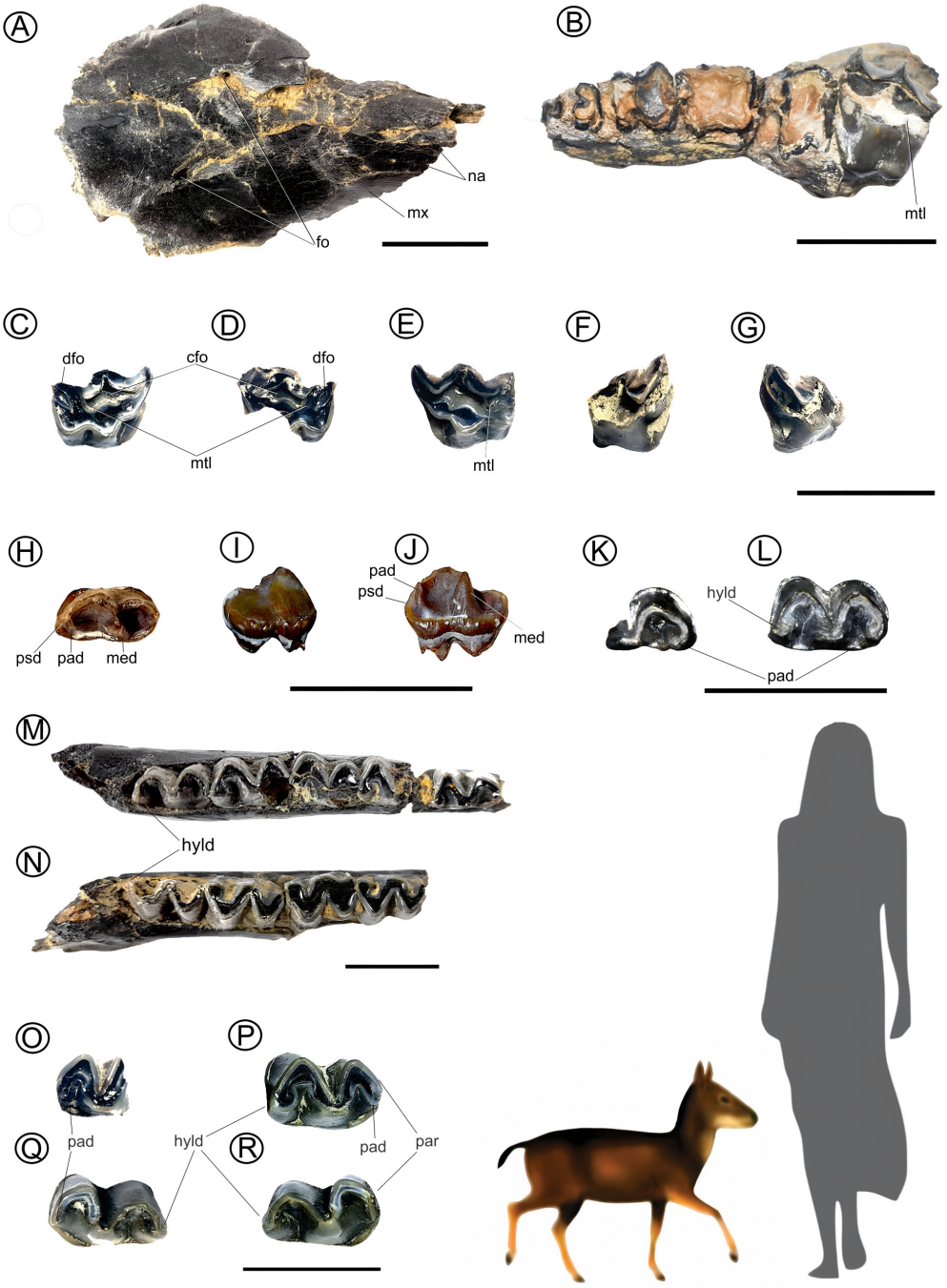

FIG. 4. ***Thoatherium minusculum***. **A.** MPM-PV 21937, skull portion (dorsal view). **B.** MPM-PV 21877, left maxillary fragment with roots of DP1-4 and M1 (occlusal view). **C-D.** MPM-PV 21899, right and left M1 (occlusal views). **E.** MPM-PV 21899, left M2 (occlusal view). **F-G.** MPM-PV 21899, right and left M3 (occlusal views). **H-J.** MPM-PV 21903, right dp2 (occlusal, buccal, and lingual views). **K-L.** MPM-PV 21900, incomplete left dp3 and dp4 (occlusal views). **M-N.** MPM-PV 21937, left mandibular fragment with p3-m3 and right one with p4-m3 (occlusal views). **O.** MPM-PV 21899, right p4. **P.** MPM-PV 21899, left m2. **Q-R.** MPM-PV 21899, right and left m3 (occlusal views). Scale bars: 20 mm. Silhouettes of proterotheriid modified from Cassini *et al*. (2012).

The dp3 of MPM-PV 21900 (Fig. 4K; Table 2) only preserves the trigonid, with a triangular buccal border at the top, rounded at its base and surrounded by a cingulid. The paralophid curves posteriorly before joining the paraconid. The lingual cingulid is faint with small crenulations. The dp4 of MPM-PV 21900 (Fig. 4L; Table 2) is more worn than dp3, with a mesiodistally shorter trigonid and a wider, slightly longer talonid. There is a small tubercle next to the paraconid, similar to dp3 (Fig. 4K, L). The metaconid is the tallest cusp. The hypolophulid ends in a well-developed hypoconulid that is roughly the same size as the paraconid. The entoconid is absent. Both the lingual and buccal flexids penetrate deep into the tooth.

The p3 of MPM-PV 21937 (Fig. 4M; Table 2) exhibits a longer and narrower trigonid compared to the talonid. The paralophid extends forward and gradually curves, ending in a rounded paraconid as large as the hypoconulid. The talonid is triangular in shape because the cristida obliqua and the hypolophulid form an acute angle. The buccal cingulid is faint, and there are two better-developed cingulids at the base of the lingual flexids, separated by a mesiodistally elongated metaconid. On the left hemimandible, the trigonid of p4, the lingual side of m1, and the lingual trigonid of m2 are broken, but these teeth remain intact on the right ramus. The teeth exhibit similar moderate wear.

The p4 of MPM-PV 21937 (Fig. 4M, N; Table 2) presents the trigonid slightly shorter and more triangular in shape. The paralophid does not extend forward and ends in a paraconid slightly less developed than the anterior tooth. The ectoflexid is deeper with a more transverse orientation. Buccal and lingual cingulids resemble those described in p3. The m1 is the most worn tooth, with the protoconid and hypoconid exhibiting a rounded border. The buccal cingulid is well-developed and presents tiny crenulations. The paraconid is not distinguishable, and the metaflexid is only a weak undulation. The hypoconulid is large, due to differential wear on the left tooth its lingual edge is straight while the same structure over the right tooth is rounded. The entoflexid is shallow. The m2 shares similar morphology and degree of wear with p4, but it is larger. The cristida obliqua is more convex and forms a wide angle with the hypolophulid. The buccal cingulid is less developed than in m1, and more prominent around the trigonid. The lingual cingulids are barely developed. The paralophid is slightly shorter than in m1 and finishes in a paraconid more buccally positioned. The hypoconulid is a large cusp. The m3 is barely worn. It is longer and narrower than the preceding teeth. The paralophid is slightly longer than in the previous teeth and ends in a very faint paraconid. The trigonid is shorter and more triangular than the talonid, with the hypolophulid extending distally and lingually, ending in a small hypoconulid (Fig. 4M, N). The ectoflexid is wide and deep resulting in a great separation between the protoconid and the hypoconid. The buccal cingulid is poorly developed. The lingual flexids also penetrate deeply, and the lingual cingulids are not visible.

The p4 of MPM-PV 21899 (Fig. 4O) preserves the trigonid and a portion of the cristida obliqua. Paralophid and metalophid are somewhat convex, while the cristida obliqua is straight. There is no buccal cingulid. The paralophid is long, projecting slightly mesially and then lingually. The paraconid is separated from the metaconid by a shallow metaflexid. The lingual cingulid projects from the paraconid to the metaconid. The ectoflexid is deep and narrow, reaching the metaconid, which is the highest cusp.

In the m2 of MPM-PV 21899 (Fig. 4P), the paralophid is slightly short and does not curve at its lingual end. The paraconid is well developed. Buccally, the ectoflexid is somewhat wider than but just as deep as in p4; a low and faint cingulid borders that side. The trigonid is shorter and narrower than the talonid. Lingually, the metaflexid is wider than that of p4. The metaconid is robust. An anterolingual cingulid extends from the paraconid to the metaconid and another short one extends from the metaconid to the base of a rounded hypoconulid.

Both m3s of MPM-PV 21899 are complete and identical in size and shape (Fig. 4Q, R). The paralophid projects mesially, curving lingually at its anterior half. The paraconid is tiny. All flexids are wide. The metaconid is tall and short. The mesiolingual cingulid extends more obliquely than in m2 and is much robust and convex. The distolingual cingulid is fainter than in m2. The cristida obliqua and the hypolophulid form a wider arch than in m2, making the talonid longer and narrower than the trigonid.

Comments: The skull fragment (MPM-PV 21937) shares with *Thoatherium minusculum* (MACN-A 9080-81, MACN-A 2996, and FMNH P 13193) a more triangular morphology than in other genera due to an anteriorly pointed snout and the presence

of more pronounced frontal grooves. The size and general morphology of the skull roof, and the morphology of both foramina and the frontal grooves are comparable to those of MACN-A 9080-81 and MACN-A 2996.

MPM-PV 21877 (DP1-4 and M1) is similar in size to *Tetramerorhinus lucarius* (MACN-A 3021, MACN-A 1855) or *Anisolophus australis* (MACN-A 3107). However, the presence of a lophoid metaconule as a transverse septum, a laterally connected protocone and hypocone, and a very deep trigon basin, similar to MPM-PV 21899, are unambiguous features of *Thoatherium minusculum* (MACN-A 3002-03, MPM-PV 3682, MPM-PV 19453, MPM-PV 3529, and YPM-VPPU 15236) (Soria, 2001; Cassini *et al*., 2012; Schmidt *et al*., 2019).

The dp2 of MPM-PV 21903 is like those of MACN-A 3000 and MACN-A 3002-03, but it differs from them because the metaconid is in a more mesial position.

The dp3-4 of MPM-PV 21900 resemble MACN-A 3000, MACN-A 3002-03, MPM-PV 19458, and MPM-PV 19459, which were assigned to *T. minusculum* (Soria, 2001; Schmidt *et al*., 2019), and the lingual tubercles next to the paraconid are also observed in MPM-PV 19459. Unlike *T. minusculum*, however, the deciduous teeth of *Tetramerorhinus lucarius* (MACN-A 1843-44) (Soria, 2001) exhibit an entoconid in dp3-4, the paralophid of dp3 does not project mesially, and the paraconid is less developed.

The morphology of the p3 in *T. minusculum* and *Tetramerorhinus* species is quite similar. However, in both p3 (MACN-A 2998-99) and dp3 (MPM-PV 21900, MPM-PV 19150, MPM-PV 19458) of *T. minusculum*, the paralophid extends somewhat more mesially and curves more abruptly near its lingual end before culminating in a rounded paraconid. The contour of the trigonid is somehow more polygonal in shape as observed in MPM-PV 21937. Distally, the talonid shows a well-developed and rounded hypoconulid, without entoconid. Both hemimandibles of MPM-PV 21937 are very similar to YPM-VPPU 15295 of *T. minusculum* (Scott, 1910; Plate II, fig. 4), and p4 and m3 are to MACN-A 9082, MPM-PV 19460, and MPM-PV 19457 of the same species (See Schmidt *et al*., 2019).

The specimens MPM-PV 21937 (left p3-m3 and right p4-m3) and MPM-PV 21899 (p4, m2-3) present a combination of features exclusively compatible with *T. minusculum*. Among them, the absence of an entoconid is only shared with specimens of *Diadiaphorus majusculus*, where this cusp appears imperfectly fused to the hypoconulid, giving it a rather triangular morphology, especially in m3. In *T. minusculum*, there is no trace of an entoconid in any of its molars, due to its loss or complete fusion with the hypoconulid. This trait, along with its small size, is unique to this species. The remaining Santacrucian species of comparable size, such as *Tetramerorhinus lucarius* and *Anisolophus australis*, retain a distinctive entoconid.

Genus ***Diadiaphorus*** Ameghino, 1887

Type species: *Diadiaphorus majusculus* Ameghino, 1887. Santa Cruz Formation (Early-Middle Miocene), Río Santa Cruz, Province of Santa Cruz, Argentina.

Diadiaphorus majusculus Ameghino, 1887
(Fig. 5A-I; Tables 1 and 2)

List of synonymies: See Soria (2001, p. 65).
Holotype: MLP-PV 12-333; right hemimandible with roots of p4, m1 partially preserved, and m2-3.
Referred material: MPM-PV 21881; right maxillary fragment with incomplete P3-P4. MPM-PV 21882; left P3 and M2 (incomplete), and right M1 (with the buccal side broken) and M3. MPM-PV 21884; left maxillary fragment with posterior root of P2 and a P3 without buccal side. MPM-PV 21902; left mandibular fragment with p3 (broken) and p4. MPM-PV 22340; incomplete right m3.
Geographic provenance: Río Chalía. MPM-PV 21881, MPM-PV 21882, MPM-PV 21884, and MPM-PV 21902 come from P8 locality; and MPM-PV 22340 was recovered from P7 locality.
Stratigraphic provenance: Santa Cruz Formation (Early-Middle Miocene, Santacrucian SALMA).
Description: The P3 MPM-PV 21881 (Fig. 5A) preserves protocone and hypocone connected by wear, although separated lingually by a subtle distolingual groove. A continuous cingulum surrounds the lingual base, which is interrupted in the P3 of MPM-PV 21882 (Fig. 5B) and MPM-PV 21884 (Fig. 5C) by the base of the protocone. In both teeth, the mesiodistal groove widens distally forming a deep, triangular-shaped fossa. In MPM-PV 21882 there is a low and poorly defined metaconule, while in MPM-PV 21884 it is absent, resulting in an uninterrupted valley.

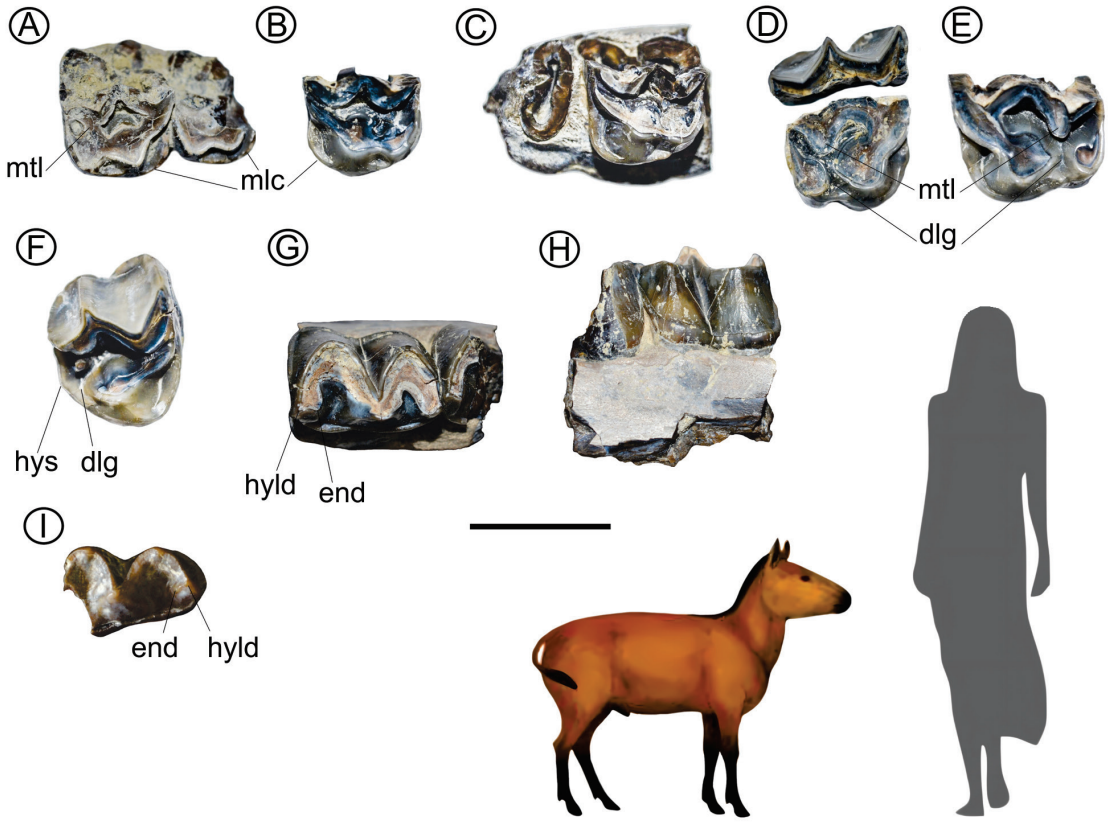

FIG. 5. ***Diadiaphorus majusculus***. **A.** MPM-PV 21881, right maxillary fragment with incomplete P3-P4 (occlusal view). **B.** MPM-PV 21882, left P3 (occlusal view). **C.** MPM-PV 21884, left maxillary fragment with posterior root of P2 and P3 without buccal side (occlusal view). **D-F.** MPM-PV 21882, left M1, right M2 (incomplete), and right M3 (occlusal views). **G-H.** MPM-PV 21902, left mandibular fragment with p3 (broken) and p4 (occlusal and buccal views). **I.** MPM-PV 22340, incomplete right m3 (occlusal view). Scale bars: 20 mm. Silhouettes of proterotheriid modified from Cassini *et al*. (2012).

The P4 MPM-PV 21881 is larger than P3 and heavily worn, exhibiting partially preserved protocone and metacone (Fig. 5A; Table 1). The metaconule is fused to the metacone and hypocone, forming a septum that separates the posterior circular distal fossette from the central fossette (Fig. 5A). The M1 (broken) and M2 (without buccal side) of MPM-PV 21882 are similar, but M1 is more worn and the cusps are connected by wear (Fig. 5D, E). The paracone is larger than the metacone, and the parastyle and mesostyle are more developed than the metastyle. Interstylar folds are absent. Similar to M2, the protocone and hypocone are separated by the distal groove. In M1-2, the metaconule is fused to the metacone. A lingual cingulum extends from the paraconule up to the hypocone. The M3 (Fig. 5F) is trapezoidal and smaller than M2 (Table 1). The parastyle is the most developed buccal style. The metaconule is small and bunoid, attached to the metacone at its base. The well-developed protocone is joined through wear to an elongated paraconule, creating a continuous surface. The mesiolingual cingulum is well developed, displaying faint crenulations along its border and forming a deep groove. The hypocone is absent, but a hypostyle develops distally, separated from the protocone by the distolingual groove (Fig. 5F).

The p3 MPM-PV 21902 (Fig. 5G, H; Table 2) only preserves a low cingulid and a less-worn hypolophulid compared to p4. The trigonid of the p4 is more triangular, shorter, narrower, and taller than the talonid.

On the buccal side, there is a deep ectoflexid. The paralophid is long and ends in a prominent paraconid. The metaflexid is shallower than the entoflexid, both resembling a shark fin in shape. The three lingual cusps are aligned at the same level and parallel to the mandibular border. The metaconid is the highest cusp slightly pointing forward. The entoconid and hypoconulid are mostly fused into a single cusp, with the entoconid representing a small protuberance pointing mesially from the hypoconulid (Fig. 5G). A basal cingulid surrounds the tooth.

The m3 MPM-PV 22340 (Fig. 5I; Table 2) is unworn and lacks its mesial portion. The trigonid is higher, shorter, and wider than the talonid. Both lingual flexids penetrate deep into the crown. The lingual cingulid exhibits weak crenulations at the base of the metaconid which is the highest cusp followed by the protoconid, hypoconid, and hypoconulid, respectively. The ectoflexid is deep. The hypolophulid ends in a well-developed hypoconulid, more buccally located than the metaconid. The entoconid is almost fused to the hypoconulid.

Comments: *Diadiaphorus majusculus* represents the largest known Santacrucian proterotheriid (Soria, 2001; Monsalvo and Costamagna, 2023). The considerable size of the dental elements (Tables 1 and 2) and the morphology described is consistent with the expected for this species. The presence of distinct features such as a rounded lingual contour, a prominent protocone and hypocone, and a well-developed mesiolingual cingulum in P3-4 (MPM-PV 21881, MPM-PV 21882, MPM-PV 21884) are typical features of *D. majusculus* as observed in specimens MACN-A 9198-99 and MLP-PV 12-305 (Soria, 2001). The fusion of metaconule and metacone due to wear in M1-2, their proximity in M3, the separation of the protocone and hypocone by a distolingual groove, the well-developed buccal styles in upper molars, and the absence of buccal folds are unambiguous characteristics also observed in specimens MACN-A 9198-99, MLP-PV 12-253, and MLP-PV 12-254 of *D. majusculus* (Soria, 2001). Furthermore, the large size of MPM-PV 22340, its prominent crown, the typical absence of an entoconid or its fusion to the hypoconulid without a tendency to form a third lobe are specific features of *D. majusculus*, as seen in MLP-PV 12-333 (holotype), MACN-A 9200-08, and MLP-PV 12-325 (Soria, 2001).

Genus ***Anisolophus*** Burmeister, 1885

Type species: *Anchitherium australe* Burmeister, 1879. Santa Cruz Formation (Early-Middle Miocene), Río Chico, Province of Santa Cruz, Argentina.
Referred species: *Anisolophus australis* (Burmeister, 1879), *A. floweri* (Ameghino, 1887), and *A. minusculus* (Roth, 1899).

Anisolophus australis (Burmeister, 1879)
(Fig. 6A-H; Table 2)

List of synonymies: See Soria (2001, p. 72).
Holotype: MACN PV 2417; incomplete palate with left P2-M3 without buccal regions, and right P2-4 badly preserved.
Referred material: MPM-PV 21898; upper incisor and left mandibular fragment with p4. MPM-PV 21878; isolated left p2, left mandibular fragment with p4-m1, and incomplete left m3. MPM-PV 21879; right mandibular fragment with broken p4, m1-2, and erupting m3.
Geographic provenance: Río Chalía, P2 locality.
Stratigraphic provenance: Santa Cruz Formation (Early-Middle Miocene, Santacrucian SALMA).
Description: The upper incisor (MPM-PV 21898) presents a very curved root with an oval cross section, being laterally compressed and wide in its middle portion (Fig. 6A). A narrow root canal can be observed at both ends of the tooth, even in the broken portion of the crown. This small proximal portion of the crown is also oval in cross section.

The p2 of MPM-PV 21878 is a small, buccally convex, and unicuspidate tooth (Fig. 6B-D; Table 2). The paralophid bifurcates into a long and more mesiolingual parastylid and a lingual paraconid (Fig. 6B, C). The protoconid and metaconid appear to form a single cusp, with the latter emitting a distolingual projection. Only part of the posterior root is preserved.

The p4s of both MPM-PV 21898 and MPM-PV 21878 show moderate wear, although the former is slightly more worn, and the buccal cusps have a more rounded outline and a less pronounced ectoflexid (Fig. 6E, F). The paralophid does not reach the lingual edge of the mandible and ends in a poorly developed paraconid. The lingual flexids are shallow and the metaconid is mesiodistally long with a distal projection towards the entoflexid.

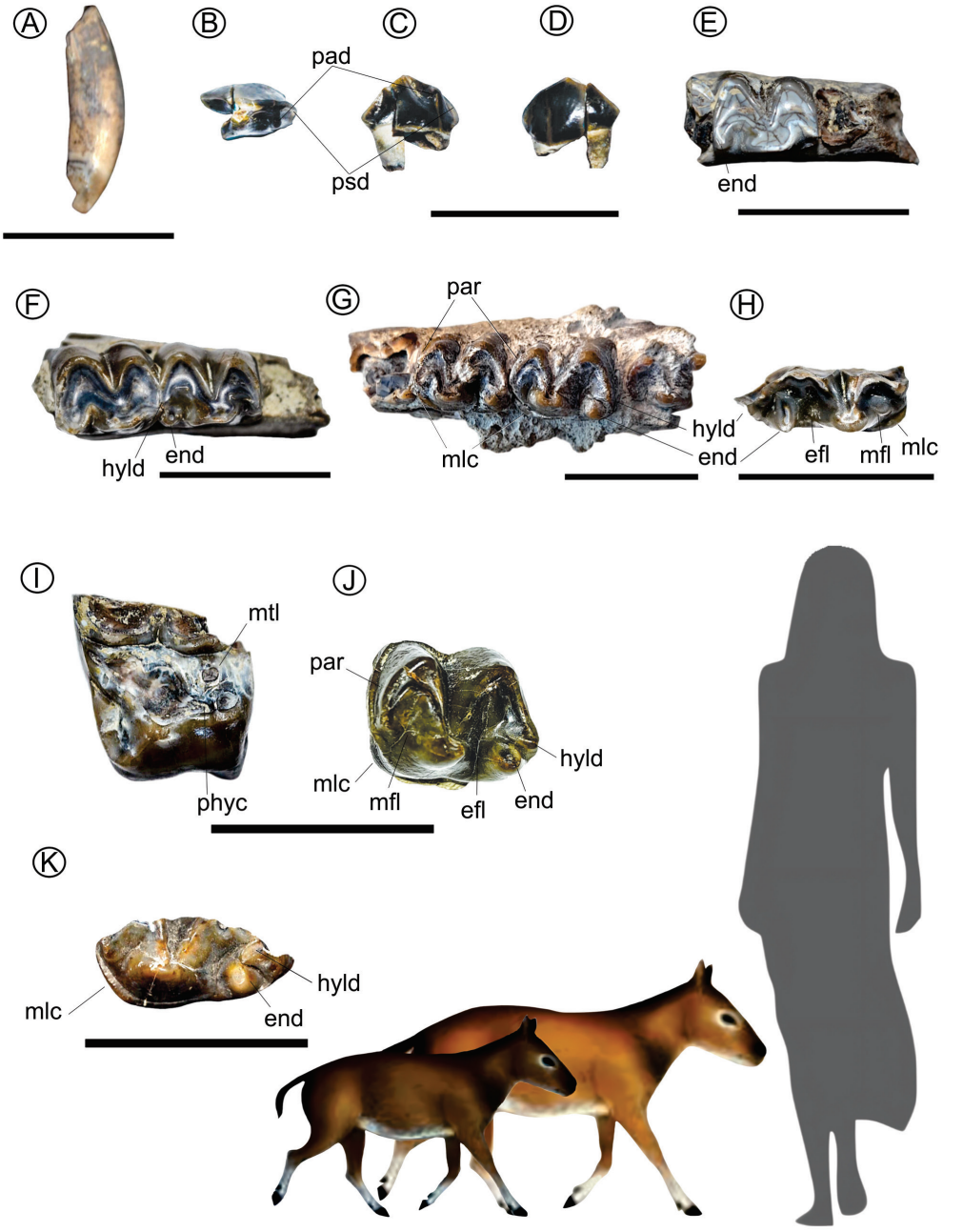

FIG. 6. ***Anisolophus australis*. A**. MPM-PV 21898, upper incisor. **B-D.** MPM-PV 21878, isolated left p2 (occlusal, lingual, and buccal views). **E.** MPM-PV 21898, left p4 (occlusal view). **F.** MPM-PV 21878, left mandibular fragment with p4-m1 (occlusal view). **G.** MPM-PV 21879, right mandibular fragment with broken p4, m1-2, and erupting m3 (occlusal view). **H.** MPM-PV 21878, left m3 (incomplete, occlusal view). ***Anisolophus floweri*. I.** MPM-PV 21880, left M2 (broken, occlusal view). **J.** MPM-PV 21905, right m2 (occlusal view). **K.** MPM-PV 21901, right m3 (incomplete, occlusal view). Scale bars: 20 mm. Silhouette of proterotheriids modified from Cassini *et al*. (2012).

The cristida obliqua is straight and projects mesiobuccally towards the metaconid. The hypolophulid ends in a small entoconid (Fig. 6E), while lesser wear reveals a small hypoconulid (Fig. 6F).

The m1 of MPM-PV 21878 is more worn than the p4 (Fig. 6F). The paraconid is absent and the paralophid is truncated by the distal wall of the p4. A buccal cingulid surrounds the trigonid. The metaflexid is lost due to wear, and a shallow entoflexid separates the metaconid from the entoconid and the hypoconulid. The buccal cusps are rounded, and the hypolophulid is straight, not curved as in p4 (Fig. 6F).

In MPM-PV 21879 the enamel is relatively thick (Fig. 6G). The trigonid of m1-2 is shorter, narrower, and higher than the talonid. The m2 shows a strong cingulid that borders the base of the trigonid. The paralophid is short and does not reach the level of the metaconid. The paraconid is absent. The ectoflexid is deep. In m1-2, the entoconid and the hypoconulid are nearly subequal in size. In occlusal view, the entoconid is more lingually placed than the hypoconulid (Fig. 6G). Both are separated by an oblique groove. The m3 has a more curved paralophid and lacks a paraconid. The talonid is broken.

Only the lingual side of the m3 of MPM-PV 21878 is preserved (Fig. 6H). The tip of the paralophid is buccally placed, indicating that it was very short. The metaflexid is shallow and higher than the entoflexid. The talonid is very long. Inside the broad entoflexid, there is a conspicuous entoconid more mesiolingually placed than the hypoconulid, which is also large but broken buccodistally.

Comments: The morphology of the upper incisors of Proterotheriidae could reflect sexual dimorphism, where robust forms could be males and more gracile forms with a circular cross-section, would correspond to females (Soria, 2001). Specimens of *A. australis*, such as YPM-VPPU 15368, show an oval cross-section proximally and a flattened cross-section distally. Because only a small portion of the proximal crown with an oval cross-section is preserved in MPM-PV 21898, it does not provide taxonomic information. However, the morphology of the p4s (MPM-PV 21898 and MPM-PV 21878) closely resembles specimens MACN-A 1861, MLP-PV 12-336, and MLP-PV 12-341, identified as *A. australis*.

The presence of a short paralophid, absence of paraconid, a thick enamel, and a well-developed entoconid observed in m1-2 of MPM-PV 21879 are typical characteristics of the genus *Anisolophus* (Soria, 2001; Schmidt *et al.,* 2019). In the molars, the position of the entoconid is similar to the premolars, but in this case, the hypoconulid is well developed and separated from the entoconid by an oblique groove. The three valid species of *Anisolophus* (*A. floweri*, *A. australis*, and *A. minusculus*) are primarily distinguished by size (Soria, 2001). In this sense, MPM-PV 21879 is compatible with *A. australis*, which is the smallest, and remarkably similar to YPM-VPPU 15996 and MPM-PV 19444. Moreover, MPM-PV 21879 presents identical measurements to the specimen MACN-A 8669 (type of the synonym of *A. australis*), although is less worn. MPM-PV 21878 is similar in size to MPM-PV 21879 but exhibits more wear, which makes it even more similar to MACN-A 8669. The morphology of the associated m3 is also comparable with the latter specimen and also to MPM-PV 19444 and MACN-A 1861. The characters observed in the p2 are also present in YPM-VPPU 15996. Based on these observations, we assign MPM-PV 21878 to *A. australis* as well.

Anisolophus floweri (Ameghino, 1887)
(Fig. 6I-K; Tables 1 and 2)

List of synonymies: See Soria (2001, p. 73).
Holotype: Right hemimandible with alveoli of p4 and m1-m3 (*fide* Ameghino, 1889). Not found. Belongs to the MLP-PV.
Referred material: MPM-PV 21880; broken left M2. MPM-PV 21905; right m2. MPM-PV 21901; lingual side of right m3.
Geographic provenance: Río Chalía. MPM-PV 21880 comes from P8 locality; MPM-PV 21905 is from P6 locality; and MPM-PV 21901 comes from P7 locality.
Stratigraphic provenance: Santa Cruz Formation (Early-Middle Miocene, Santacrucian SALMA).
Description: The M2 of MPM-PV 21880 is partially preserved (Fig. 6I). It is a heavily worn, low-crowned tooth**.** The trigon basin is shallow. The protocone and hypocone are laterally connected by an enamel ridge (prehypocrista; Püschel *et al*., 2024) (Fig. 6I). There is a smooth concavity separating them at their base, but the distolingual groove is absent. The metaconule is bunoid, closer to the hypocone, but separated from it by a groove. The protocone is the largest cusp and is joined to a prominent paraconule by a surface of wear. The lingual side

of the tooth is almost straight, and a well-developed mesiolingual cingulum contributes to its quadrangular shape. The lingual cingulum is lacking.

The m2 of MPM-PV 21905 has a thick enamel (Fig. 6J). The trigonid is smaller than the talonid, and the corresponding metaflexid is shallower than the entoflexid. The cingulids are not continuous. Only the mesial and the buccal wall of the trigonid and the distal wall of the talonid show a cingulid at the base. The paraconid and the hypoconid show a triangular outline at their apices in occlusal view, but the base of both cusps is rounded. The paralophid is short, mesially curved, and without a paraconid (Fig. 6J). The metalophid also curves mesially, reaching the metaconid which is the highest cusp. The cristida obliqua projects straight from the hypoconid to the metaconid. Both metalophid and cristida obliqua form a deep ectoflexid. Although the mesial wall of the tooth is straight at the base, the hypolophulid is slightly concave at the top and ends in the hypoconulid which is subequal in size to the entoconid, the latter being taller and more mesiolingually placed than the hypoconulid. Both cusps are separated by a well-defined groove that penetrates into the entoflexid.

The m3 of MPM-PV 21901 is broken on the buccal side (Fig. 6K). The preserved element exhibits no wear. It lacks a paraconid, the paralophid is short, and the metaflexid is very shallow. The entoconid is well developed (Fig. 6K). The lingual cingulid extends from the paralophid to the metaconid, with greater development at the entrance of the metaflexid forming a sort of crest. The metaflexid is relatively shallow.
Comments: The characteristics observed in the M2 of MPM-PV 21880, such as the low crown, a wide and shallow trigon basin, rounded cusps, a metaconule positioned closer to the hypocone, a protocone connected to the hypocone by an enamel ridge, and the absence of a distolingual groove, are exclusive features of the genus *Anisolophus* (Soria, 2001; Schmidt *et al*., 2019). In addition to the difference in size, the assignment of MPM-PV 21880 to *A. australis* is discarded because the posterolingual groove is less marked than in MACN-PV 2417 (holotype of *A. australis*). MPM-PV 21880 also exhibits a close resemblance to the upper teeth of MPM-PV 19429, MACN-A 9003-12, and MACN-A 3098, all assigned to *A. floweri*.

Regarding the lower dentition, the m2 of MPM-PV 21905 is morphologically similar to MPM-PV 21879 (assigned to *A. australis*), but is considerably larger (Table 2), with a better-developed entoconid and thicker enamel. MPM-PV 21905 is very similar in shape and size to YPM-VPPU 15309 and MLP-PV 12-289, assigned to *A. floweri*, where the cingulid encloses the trigonid without surpassing the metaconid at the lingual side.

In m3 (MPM-PV 21901), the short paralophid without paraconid, the shallow metaflexid, the thick enamel, and the low metaconid are all indicative of the genus *Anisolophus*. The tooth is almost identical in shape and size to MPM-PV 19432 and MPM-PV 19442 of *A. floweri*. Therefore, we assign this tooth to this species.

Family Macraucheniidae Gervais, 1855
Subfamily Cramaucheniinae Ameghino, 1902
Genus ***Theosodon*** Ameghino, 1887

List of synonymies: See Soria (1981, p. 18).
Type species: *Theosodon lydekkeri* Ameghino, 1887. Santa Cruz Formation (Early-Middle Miocene), Río Santa Cruz, Province of Santa Cruz, Argentina.
Referred species: *Theosodon lydekkeri*, *T. lallemanti*, *T. garrettorum*, *T. fontanae*, *T. gracilis*, *T. patagonicum*, *T. karaikensis*, *T. pozzii*, *T.*? *frenguellii*, and "*Theosodon*" *arozquetai*.

Theosodon sp.
(Fig. 7A-F; Tables 1 and 2)

Referred material: MPM-PV 21876; left P3. MPM-PV 21883; left mandibular fragment with dp3. MPM-PV 21875; left calcaneus.
Geographic provenance: Río Chalía. MPM-PV 21876 comes from P2 locality; MPM-PV 21883 is from P8 locality; and MPM-PV 21875 comes from P7 locality.
Stratigraphic provenance: Santa Cruz Formation (Early-Middle Miocene, Santacrucian SALMA).
Description: The buccal side of MPM-PV 21876 (P3), consists of a single and straight lobe surrounded by a continuous cingulum that forms the parastyle (mesially) and metastyle (distally), and a central paracone (Fig. 7A, B). The lingual wall is rounded, slightly lower than the buccal, and the protocone is mesially placed. A median longitudinal valley runs mesiodistally, opening near the parastyle. Distally, it widens and deepens, becoming a median fossette close to the posterior wall.

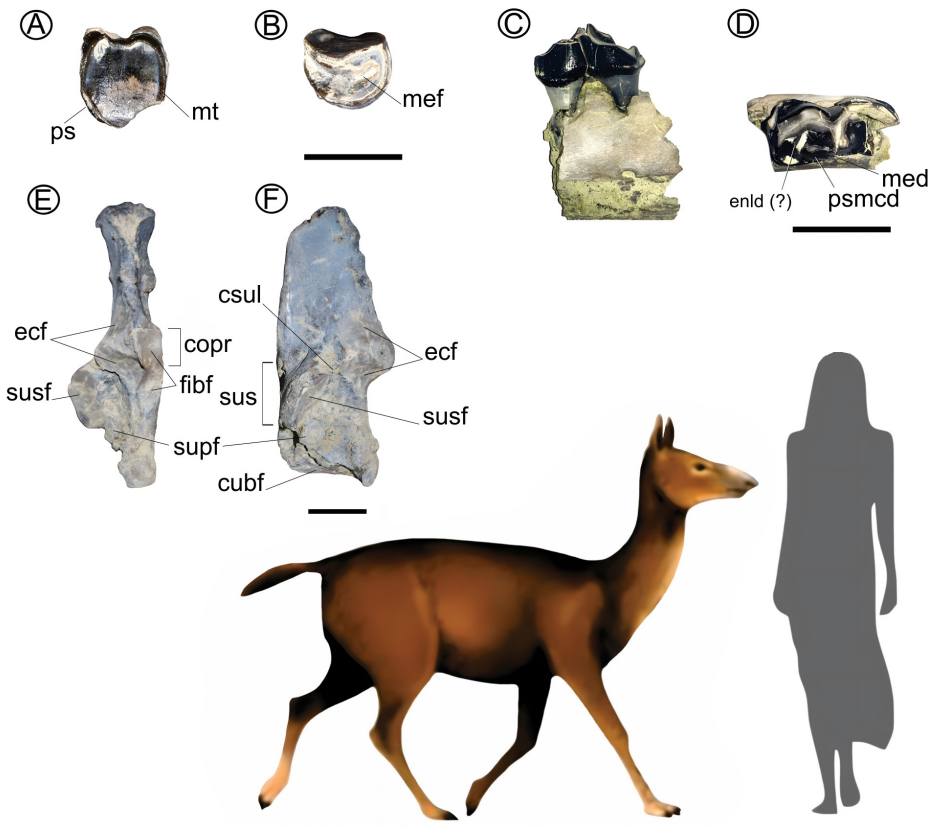

FIG. 7. ***Theosodon* sp. A-B.** MPM-PV 21876, left P3 (buccal and occlusal views). **C-D.** MPM-PV 21883, left mandibular fragment with dp3 (buccal and occlusal views). **E-F.** MPM-PV 21875, left calcaneus (dorsal and medial views). Scale bars: 20 mm. Silhouette of macraucheniid modified from Cassini *et al*. (2012).

The dp3 of MPM-PV 21883 (Fig. 7C, D) is elongated mesiodistally and biradiculated. The ectoflexid is shallow. The trigonid is mesially broken and longer than the talonid. A buccal and basal cingulum surrounds the crown, expanding distally. On the lingual side, the metaconid is well-developed, with a short distal projection forming a lingual buttress (postmetacristid; Püschel *et al*., 2024). In the talonid, a faint entolophid is present (Fig. 7D).

The body of the calcaneus (MPM-PV 21875; Fig. 7E, F) is lateromedially compressed. The dorsal border is thinner than the plantar one, and the proximal end is broken, resulting in the absence of the tuber calcis. In lateral view, the dorsal outline is almost straight, while the plantar one is slightly curved. The coracoid process has a rounded dorsal outline. In dorsal view (Fig. 7E), the fibular facet is broad and is delimited by two subparallel borders. Laterally, it forms a slide-like concavity. Distal to this concavity, the dorsal border projects upwards, increasing the height towards the facet for the cuboid. The ectal and the sustentacular facets are separated by a narrow but well-defined calcaneal sulcus (Fig. 7F). The sustentaculum is large, spoon-shaped, and bears a slightly concave sustentacular facet for the astragalus. Distal to the latter and separated from it, there is a rounded supplementary facet for the astragalus that faces more mesially. Finally, the distal end of the calcaneus is compressed lateromedially.

Comments: The shape and size of the P3 MPM-PV 21876 coincide with the genus *Theosodon*, particularly resembling YPM-VPPU 15164 (holotype of *Theosodon garrettorum*), MPM-PV 17481 (*Theosodon* cf. *lydekkeri*), MPM-PV 19202

(assigned to *Theosodon* sp.), and UATF-V-001940 ("*Theosodon*" *arozquetai*) (Scott, 1910; McGrath *et al.,* 2018). It differs from other Cramaucheniinae such as *Cramauchenia normalis* (MPEF-PV 2524; Dozo and Vera, 2010) due to its smaller size and more triangular shape.

MPM-PV 21883 is remarkably similar to the dp3 of YPM-VPPU 016002, depicted as *Theosodon lallemanti* (Scott, 1910; Plate XVIII, fig. 1). Although slightly more worn, the lingual buttress of the metaconid is still visible, while the entolophid is not. The proportion of both lobes is quite similar, although the distobuccal cingulum is more expanded. MPM-PV 21883 is also similar to MACN-A 9269-88 of *T. lydekkeri* (see Cassini *et al*., 2012). However, in this case, the distobuccal cingulum is nearly identical.

The first upper premolars in *Theosodon* spp. are relatively simple morphologically, without features that allow us a reliable determination at a specific level. The same occurs with the lower deciduous premolar (dp3). Hence, we consider the assignment of specimens MPM-PV 21876 and MPM-PV 21883 as *Theosodon* sp. as the most appropriate.

The smaller size, gracefulness, and absence of the tuber calcis in the calcaneus MPM-PV 21875 indicate a young individual. According to Scott (1910), the only macraucheniid recorded from the SCF is *Theosodon*. The second larger litoptern present in this formation is the Proterotheriidae *Diadiaphorus majusculus*. Despite MPM-PV 21875 is a young specimen, it is even larger than the calcaneus of adult individuals of *D. majusculus* such as AMNH 9270. In addition to size, MPM-PV 21875 differs from AMNH 9270 because the body is less elongated, with non-subparallel dorsal and plantar borders as observed in *D. majusculus*. The tuber calcis is absent in MPM-PV 21875, but part of the suture is preserved. In medial view, it describes a straight line that forms an obtuse angle with respect to the plantar edge. Conversely, in *D. majusculus*, this line is sinuous and more vertically oriented. The coracoid process is larger and more rounded in *Theosodon* than in *D. majusculus*, and there is a more pronounced anterior concavity in front of it, as in MPM-PV 21875. In *Theosodon*, the sustentaculum is spoon-like shaped with a sharp mesial border, whereas in *D. majusculus*, the border of this structure is blunt and thick and the sustentacular facet points upwards rather than forward and mesially, being less visible in mesial view compared to *Theosodon*. Additionally, in MPM-PV 21875, there is a rounded and isolated supplementary facet for the astragalus. This feature is very clear in the specimen MACN A-9269-88. In *Diadiaphorus* and proterotheriids in general, there is a continuous sustentacular facet or a very small supplementary facet. In *Theosodon*, the calcaneal sulcus is typically more excavated, so there is a clearer separation between the ectal and the sustentacular facets. In lateral view, the distal portion of the calcaneus is higher, and the anterior process above the facet for the cuboid points upwards, contrasting with the horizontal or even downward orientation observed in *D. majusculus* (AMNH 9270, MACN-A 1816-17-19). Considering the differences between the calcaneus MPM-PV 21875 with those of the larger Santacrucian proterotheriid *D. majusculus*, and the similarity observed with the specimens MACN-A 9269-88 and MACN-PV 17625, determined as *Theosodon* sp., it is appropriate to assign MPM-PV 21875 to *Theosodon* sp.

5. Discussion

Soria (2001) identified four species from the Río Chalía based on MACN specimens (see Appendix), *Anisolophus floweri, A. minusculum, Tetramerorhinus cingulatum*, and *Te. mixtum*. In the new litoptern collection reported here, we identified five genera and, at least, seven species: six proterotheriids (*Te. lucarius*, *Te. cingulatum*, *Thoatherium minusculum*, *Diadiaphorus majusculus*, *A. floweri*, and *A. australis*,) and one macraucheniid (*Theosodon* sp.). We did not identify *A. minusculum* nor *Te. mixtum*, so the validity of these species is still under revision.

As mentioned above, the specimens collected at the Río Chalía were referred to three altitudinal levels (A, B and C) that cover the whole section of the SCF (~18-15.2 Ma). The taxonomic distribution of proterotheriids from the Río Chalía, collected with precise altitudinal information, reveals some differences that may be related to body size, with a predominance of larger species of each genus at lower stratigraphic levels (Table 3). *Anisolophus floweri* and *Tetramerorhinus cingulatum* are found in level A but not in level C, while *A. australis* and *Te. lucarius* are recorded in level C. *Diadiaphorus majusculus*, the largest proterotheriid of the SCF, is recorded only in level A. *Thoatherium minusculum*, the smallest form, is recorded in both levels A and C

TABLE 3. DISTRIBUTION OF THE LITOPTERN TAXA RECORDED AT THE RÍO CHALÍA BY LOCALITY AND ALTITUDINAL RANGE.

Altitudinal range	Taxon	MPM-PV	Locality
C 350-400 m a.s.l.	*Tetramerorhinus lucarius*	21907	P2
	Thoatherium minusculum	21899	P2
	Anisolophus australis	21898	P2
	Theosodon sp.	21876	P2
B 250-350 m a.s.l.	*Anisolophus australis*	21878, 21879	P2
	Anisolophus floweri	21905	P6
	Theosodon sp.	21875	P7
A 150-250 m a.s.l.	*Tetramerorhinus cingulatum*	21874	P7
	Thoatherium minusculum	21877, 21900, 21903, 21937	P2, P3, P6, P8
	Diadiaphorus majusculus	21881, 21882, 21884, 21902, 22340	P7, P8
	Anisolophus floweri	21880, 21901	P7, P8
	Theosodon sp.	21883	P8

but is more abundant in level A. These differences could result from sampling bias, as fewer specimens have been recovered from level C than from level A. However, the possibility that they reflect ecological or environmental changes IS worth to be explored in the future, as faunal changes related to stratigraphic provenance involving other taxa (*e.g*., frogs, rodents, and typotheres) have been reported (Kay *et al.,* 2021; Vizcaíno *et al.,* 2021; Muzzopappa *et al.,* 2025).

Based on the presence/absence of species, Río Chalía does not exhibit significant differences when compared to other exposures of the SCF elsewhere (Table 4). Combining the new specimens presented in this contribution with the previous reports of Soria (2001), the SCF at the Río Chalía contains all the species reported at the localities along the Río Santa Cruz, the Atlantic coast, and the area of Lago Posadas, except the species of *Theosodon*. When comparing the taxonomic richness at the Río Chalía and the Río Santa Cruz, both share the same species, but there are subtle differences at localities such as Segundas Barrancas Blancas and Barrancas Blancas (Schmidt *et al*., 2019) (Table 4). The taxonomic richness at the Río Chalía is more similar to Segundas Barrancas Blancas than to Barrancas Blancas, as they share five species of proterotheriids: *Anisolophus floweri*, *Tetramerorhinus lucarius*, *Te. cingulatum*, *Thoatherium minusculum*, and *Diadiaphorus majusculus*, and the genus *Theosodon*. Río Chalía and Barrancas Blancas share four species: *A. australis*, *Te. lucarius*, *Th. minusculum*, and *D. majusculus*, and the genus *Theosodon*. The major difference is that *A. floweri* and *Te. cingulatum* are both present at the Río Chalía and Segundas Barrancas Blancas but are absent at Barrancas Blancas. Conversely, *A. australis* was reported for the Río Chalía and Barrancas Blancas but was not recorded in Segundas Barrancas Blancas. All the taxa reported for the Río Chalía are also found at the Atlantic coast localities, so the only difference with Segundas Barrancas Blancas is the absence of *A. australis* in the latter. These results align with those presented by Cuitiño *et al.* (2016, 2019a), which asserted that Segundas Barrancas Blancas exhibits a higher degree of similarity in terms of taxonomic richness with the Atlantic coast (between Monte León and Río Gallegos) than with Barrancas Blancas, even though the latter two regions are closer in age than Segundas Barrancas Blancas.

Soria (2001) reported *Anisolophus minusculum* for the Río Chalía and the Atlantic coast at Monte Observación (Cerro Observatorio) and La Cueva (Cerro Monte Observación; see Marshall, 1976, and Vizcaíno *et al*., 2012b). This author also reported *Tetramerorhinus mixtum* for the Río Chalía, for the middle course of the Río Santa Cruz, and the area of Lago Posadas (Cuitiño *et al*., 2019b). The same species was reported for the Atlantic coast at Puesto Estancia La Costa (Cassini *et al*., 2012). The SCF at the Río Chalía and the area of Lago Posadas share the following taxa: *Thoatherium*

TABLE 4. RECORDS OF LITOPTERNA IN THE SANTA CRUZ FORMATION AT DIFFERENT LOCALITIES IN THE SANTA CRUZ PROVINCE.

	Atlantic coast	Río Santa Cruz[3]	Río Santa Cruz[4]		Lago Posadas	Río Chalía	Río Chalía (this paper)		
TAXA			**BB**	**SBB**			**P2/3**	**P6**	**P7/8**
Anisolophus australis	X[1]	X	X				X		
A. floweri	X[1]	X		X	X[5]	X[1]		X	X
A. minusculum	X[1]					X[1]			
Tetramerorhinus lucarius	X[1]		X	X	X[5]		X		
Te. cingulatum	X[1,2]			X		X[1]			X
Te. mixtum	X[1]				X[1]	X[1]			
Thoatherium minusculum	X[2]	X	X	X	X[1]		X	X	X
Diadiaphorus majusculus	X[2]	X	X	X					X
Theosodon lydekkeri	X[2]	X							
The. garretorum	X[2]								
The. gracilis	X[2]								
The. lallemanti	X[2]								
Theosodon sp.			X	X	X		X		X

[1]Soria (2001); [2]Cassini *et al*. (2012); [3]Ameghino (1887); [4]Schmidt *et al*. (2019); [5]Cuitiño *et al*. (2019b). **BB**: Barrancas Blancas locality at Río Santa Cruz; **SBB:** Segundas Barrancas Blancas locality at Río Santa Cruz; **P2/3**, **P6** and **P7/8:** localities at Río Chalía.

minusculum, *Tetramerorhinus lucarius*, *Te. mixtum*, and *Anisolophus floweri* (Soria, 2001; Cuitiño *et al*., 2019b). Because *Diadiaphorus* is an almost monotypic genus, except for the species *D*? *caniadensis* from the Pinturas Formation, *D. majusculus* could be present at Lago Posadas since a maxillary fragment with broken teeth (MPM-PV 17468) was assigned to cf. *Diadiaphorus* by Cuitiño *et al*. (2019b). The area of Lago Posadas presents the lowest taxonomic richness and the less similarity with Río Chalía, since the species *Te. cingulatum*, *A. australis*, and *A. minusculum* are not present, and the presence of *D. majusculus* is still uncertain.

6. Conclusions

The recovery of new litoptern remains from localities along the Río Chalía (also known as Sehuen or Shehuen) provided an opportunity to revisit the taxa recovered by C. Ameghino in 1890, some of which were identified as type specimens by F. Ameghino in later works. In this new collection, we identified six proterotheriids (*Tetramerorhinus lucarius*, *Te. cingulatum*, *Thoatherium minusculum*, *Diadiaphorus majusculus*, *Anisolophus floweri*, and *A. australis*). Regarding macraucheniids, several species of *Theosodon* were recognized for the SCF, including one from the Río Chalía (*T. fontanae*), but these taxa are still pending of a full revision. The fragmentary nature of the recovered remains allowed us to assign them only to a generic level. Litoptern taxa from the Río Chalía do not differ from those recovered at the Río Santa Cruz, as well as those from other sites across the widespread distribution of the Santa Cruz Formation. These recent collections, with precise geographic provenance and altitudinal reference may be useful in verifying Ameghino's original descriptions and revisiting the Santacrucian taxa. They also call attention to the importance of revising recent collections, particularly those from the Río Santa Cruz, to test for stratigraphic differences in association with climatic and environmental changes.

Acknowledgements

We thank the collection managers of the Vertebrate Paleontology collections at MLP: M. de Los Reyes; MACN: A. Martinelli, M. Ezcurra, and M.B. von Baczko; YPM: V. Rhue. Special thanks to S. Hernández Del Pino

and G. Cassini for sharing several photos for comparison. We are also grateful to M.E. Pérez, N.A. Muñoz, R. Tomassini, R.F. Kay, J.I. Cuitiño, M.S. Raigemborn, and B. Zorzit for their participation in the field work. We extend our appreciation to all the people in the settlements of the study area for their permission and hospitality. Thanks to the Dirección de Patrimonio Cultural of Santa Cruz Province for granting permission for explorations and fossil collection. We also thank to J.E. Bostelmann and A. Solórzano for their critical and constructive comments. D. Bertin and A. Encinas provided a final review and editorial guidance. This is a contribution to the projects PICT 2017-1081 (M.S. Bargo) and UNLP 11/N997 (S.F. Vizcaíno).

References

Ameghino, F. 1887. Enumeración sistemática de las especies de mamíferos fósiles coleccionadas por Carlos Ameghino en los terrenos eocenos de la Patagonia austral. Boletín del Museo de La Plata 1: 1-26.

Ameghino, F. 1889. Contribución al conocimiento de los mamíferos fósiles de la República Argentina. Actas de la Academia Nacional de Ciencias de Córdoba 6: 1-1027.

Ameghino, F. 1891. Nuevos restos de mamíferos fósiles descubiertos por Carlos Ameghino en el Eoceno inferior de la Patagonia austral. Especies nuevas, adiciones y correcciones. Revista Argentina de Historia Natural 1: 289-328.

Ameghino, F. 1894. Enumération synoptique des espéces des mammiferes fósiles des formations éocenes de Patagonie. Boletín de la Academia Nacional de Ciencias de Córdoba 13: 259-452.

Ameghino, F. 1899. Sinopsis geológico-paleontológica. Suplemento (Adiciones y correcciones). Imprenta La Libertad La Plata 1-13.

Ameghino, F. 1902. Premiere contribution a la connaisance de la faune mammalogique des couches a Colpodon. Boletín de La Academia Nacional de Ciencias de Córdoba 17: 71-138.

Bai, B.; Meng, J.; Wang, Y.Q.; Wang, H.B.; Holbrook, L. 2017. Osteology of The Middle Eocene Ceratomorph *Hyrachyus modestus* (Mammalia, Perissodactyla). Bulletin of the American Museum of Natural History: 1-70.

Bärmann, E.V.; Rössner, G.E. 2011. Dental nomenclature in Ruminantia: Towards a standard terminological framework. Mammalian Biology 76: 762-768. https://doi.org/10.1016/j.mambio.2011.07.002

Bond, M.; Cerdeño, E.; López, G. 1995. Los ungulados nativos de América del Sur. *In* Evolución biológica y climática de la región Pampeana durante los últimos cinco millones de años. Un ensayo de correlación con el Mediterráneo occidental (Alberdi, M.T.; Leone, G.; Tonni, E.P.; editors). Monografías del Museo Nacional de Ciencias Naturales, CSIC: 259-275. Madrid.

Bond, M.; Perea, D.; Ubilla, M.; Tauber, A. 2001. *Neolicaphrium recens* Frenguelli, 1921, the only surviving Proterotheriidae (Litopterna, Mammalia) into the South American Pleistocene. Palaeovertebrata 30 (1-2): 37-50.

Bondesio, P.; Rabassa, J.; Pascual, R.; Vucetich, M.G.; Scillato-Yane, G. 1980. La Formación Collón Cura de Pilcaniyeu Viejo y sus alrededores (Río Negro, República Argentina). Su antigüedad, y las condiciones ambientales según su distribución, su litogénesis y sus vertebrados. *In* Congreso Argentino de Paleontología y Bioestratigrafía, No. 2 y Congreso Latinoamericano de Paleontología, No. 1, Actas 3: 85-99. Buenos Aires.

Bostelmann, J.E.; Le Roux, J.P.; Vásquez, A.; Gutiérrez, N.M.; Oyarzún, J.L.; Carreño, C.; Torres, T.; Otero, R.; Llanos, A.; Fanning, C.M.; Hervé, F. 2013. Burdigalian deposits of the Santa Cruz Formation in the Sierra Baguales, Austral (Magallanes) Basin: age, depositional environment and vertebrate fossils. Andean Geology 40 (3): 458-489. https://doi.org/10.5027/andgeoV40n3-a04

Buckley, M. 2015. Ancient collagen reveals evolutionary history of the endemic South American 'ungulates'. Proceedings of the Royal Society B 282: 9 p. https://doi.org/10.1098/rspb.2014.2671

Buldrini, K.E. 2017. Los mamíferos fósiles de Pampa Guadal, Región de Aysén, Chile. Thesis. Universidad de Chile, Facultad de Ciencias: 175 p.

Buldrini, K.E.; Bostelmann, J.E. 2017. Importancia paleobiogeográfica del ensamble de ungulados miocenos de Pampa Guadal, Región de Aysén. *In* Reunión de Paleontología de Vertebrados de Chile, No. 1, (Rubilar-Rogers, D.; Otero, R.; editors). Libro de Resúmenes: p. 39.

Burmeister, G. 1879. Description physique de la République Argentine. D'après des observations personnelles et étrangères. Imprenta Paul-Émile Coni: 553 p. Buenos Aires.

Burmeister, G. 1885. Examen crítico de los mamíferos y reptiles fósiles denominados por D. Augusto Bravard y mencionados en su obra precedente. Anales del Museo Nacional de Buenos Aires 3: 95-174.

Cassini, G.H.; Cerdeño, E.; Villafañe, A.L.; Muñoz, N.A. 2012. Paleobiology of Santacrucian native ungulates (Meridiungulata: Astrapotheria, Litopterna, and Notoungulata). *In* Patagonia: High-Latitude Paleocommunities of the Santa Cruz Formation

(Vizcaíno, S.F.; editor). Cambridge University Press: 243-286. Cambridge.

Cifelli, R.L. 1983. The origin and affinities of the South American Condylarthra and early Tertiary Litopterna (Mammalia). American Museum Novitates 2772:1-49.

Cifelli, R.L.; Villarroel, C. 1997. Paleobiology and affinities of *Megadolodus*. *In* Vertebrate Paleontology in the Neotropics: The Miocene Fauna of La Venta, Colombia (Kay, R.F.; Madden, R.H.; Cifelli, R.L.; Flynn, J.J.; editors). Smithsonian Institution Press 265-288. Washington, D.C.

Corona, A.; Perea, D.; Ubilla, M. 2018. The humerus of Proterotheriidae (Mammalia, Litopterna) and its systematic usefulness: the case of "*Proterotherium berroi*" Kraglievich, 1930. Ameghiniana 55 (2):150-161. https://doi: 10.5710/AMGH.10.12.2017.3148

Corona, A.; Badín, A.C.; Perea, D.; Ubilla, M.; Schmidt, G.I. 2020. A new genus and species and additional reports of South American native ungulates Proterotheriidae (Mammalia, Litopterna) in the Late Miocene of Uruguay. Journal of South American Earth Sciences 102: 102646. https://doi: 10.1016/j.jsames.2020.102646

Croft, D.A.; Flynn, J.J.; Wyss, A.R. 2004. Notoungulata and Litopterna of the early Miocene Chucal Fauna, Northern Chile. Fieldiana Geology 50: 1-52.

Croft, D.A.; Gelfo, J.N.; López, G.M. 2020. Splendid innovation: The extinct South American native ungulates. Annual Review of Earth and Planetary Sciences 48 (1): 259-290. https://doi.org/10.1146/annurev-earth-072619-060126

Cuitiño, J.I.; Fernicola, J.C.; Kohn, M.; Trayler, R.; Naipauer, M.; Bargo, M.S.; Kay, R.F.; Vizcaíno, S.F. 2016. U-Pb geochronology of the Santa Cruz Formation (early Miocene) at the Río Bote and Río Santa Cruz (southernmost Patagonia, Argentina): implications for the correlation of fossil vertebrate localities. Journal of South American Earth Sciences 70: 198-210.

Cuitiño, J.I.; Fernicola, J.C.; Raigemborn, M.S.; Krapovickas, V. 2019a. Stratigraphy and depositional environments of the Santa Cruz Formation (early-middle Miocene) along the Río Santa Cruz, Southern Patagonia, Argentina. Publicación Electrónica de la Asociación Paleontológica. Argentina 19: 14-33.

Cuitiño, J.I.; Vizcaíno, S.F.; Bargo, M.S.; Aramendía, I. 2019b. Sedimentology and fossil vertebrates of the Santa Cruz Formation (early Miocene) in Lago Posadas, southwestern Patagonia, Argentina. Andean Geology 46 (2): 383-420. http://dx.doi.org/10.5027/andgeoV46n2-3128

Cuitiño, J.I.; Raigemborn, M.S.; Bargo, M.S.; Vizcaíno, S.F.; Muñoz, N.A.; Kohn, M.J.; Kay, R.F. 2021. Insights on the controls on floodplain-dominated fluvial successions: a perspective from the early-middle Miocene Santa Cruz Formation in Río Chalía (Patagonia, Argentina). Journal of the Geological Society 178: jgs2020-188. https://doi.org/10.1144/jgs2020-188

De la Cruz, R.; Suárez, M. 2006. Geología del área Puerto Guadal-Puerto Sánchez, Región Aisén del General Carlos Ibáñez del Campo. Servicio Nacional de Geología y Minería, Carta Geológica de Chile, Serie Geológica Básica 95: 58 p., 1 mapa escala 1:100.000. Santiago.

Dozo, M.T.; Vera, B. 2010. First skull and associated postcranial bones of Macraucheniidae (Mammalia, Litopterna) from the Deseadan SALMA (late Oligocene) of Cabeza Blanca (Chubut, Argentina). Journal of Vertebrate Paleontology 30: 1818-1826.

Fernicola, J.C.; Cuitiño, J.; Vizcaíno, S.F.; Bargo, M.S.; Kay, R.F. 2014. Fossil localities of the Santa Cruz Formation (early Miocene, Patagonia, Argentina) prospected by Carlos Ameghino in 1887 revisited and the location of the Notohippidian. Journal of South America Earth Sciences 52: 94-107. https://doi.org/10.1016/j.jsames.2014.02.002

Fernicola, J.C.; Bargo, M.S.; Vizcaíno, S.F.; Kay, R.F. 2019. Early-Middle Miocene Paleontology in the Río Santa Cruz, Southern Patagonia, Argentina. 130 years since Ameghino, 1887. Special Issue Publicación Electrónica de la Asociación Paleontológica Argentina 19 (2): 1-259.

Fleagle, J.G.; Perkins, M.E.; Heizler, M.T.; Nash, B.; Bown, T.M.; Tauber, A.A.; Dozo, M.T.; Tejedor, M.F. 2012. Absolute and relative ages of fossil localities in the Santa Cruz and Pinturas Formations. *In* Early Miocene Paleobiology in Patagonia: High-Latitude Paleocommunities of the Santa Cruz Formation (Vizcaíno, S.F.; Kay, R.F.; Bargo, M.S; editors). Cambridge University Press: 41-58. Cambridge, UK.

Forasiepi, A.M.; MacPhee, R.D.E.; Hernández del Pino, S.; Schmidt, G.I.; Amson, E.; Grohé, C. 2016. Exceptional skull of *Huayqueriana* (Mammalia, Litopterna, Macraucheniidae) from the late Miocene of Argentina: anatomy, systematics, and paleobiological implications. Bulletin of the American Museum of Natural History 404: 1-76. https://doi.org/10.1206/0003-0090-404.1.1

Gervais, P. 1855. Recherches sur les mamifères fossiles de l'Amérique du Sud. *In* Expédition dans les parties centrales de l'Amérique du Sud, de Rio de Janeiro à Lima au Para; exécuté par ordre du Gouvernement

français pendant les années 1843 à 1847 sous la direction du comte Francis de Castelnau (Castelnau, F.; editor). Zoologie 7: 1-63.

Ginot, S.; Hautier, L.; Marivaux, L.; Vianey-Liaud, M. 2016. Ecomorphological analysis of the astragalo-calcaneal complex in rodents and inferences of locomotor behaviours in extinct rodent species. PeerJ 4. https://doi.org/10.7717/peerj.2393

Harbers, H.; Neaux, D.; Ortiz, K.; Blanc, B.; Laurens, F.; Baly, I.; Callou, C.; Schafberg, R.; Haruda, A.; Lecompte, F.; Casabianca, F.; Studer, J.; Renaud, S.; Cornette, R.; Locatelli, Y.; Vigne, J.-D.; Herrel, A.; Cucchi, T. 2020. The mark of captivity: plastic responses in the ankle bone of a wild ungulate Sus scrofa. Royal Society Open Science 7 (3): 192039.

Kay, R.F.; Vizcaíno, S.F.; Bargo, M.S. 2012. A review of the paleoenvironment and paleoecology of the Miocene Santa Cruz Formation. *In* Early Miocene Paleobiology in Patagonia (Vizcaíno, S.F.; Kay, R.F.; Bargo, M.S.; editors). Cambridge University Press: 331-365. Cambridge.

Kay, R.F.; Vizcaíno, S.F.; Bargo, M.S.; Spradley, J.S.; Cuitiño, J.I. 2021. Paleoenvironments and paleoecology of the Santa Cruz Formation (Early-Middle Miocene) along the Río Santa Cruz, Patagonia. Journal of South American Earth Sciences 109. https://doi.org/10.1016/j.jsames.2021.103296

Kerber, L.; Kinoshita, A.; José, F.A.; Graciano Figueiredo, A.M.; Oliveira, E.V.; Baffa, O. 2011. Electron spin resonance dating of the southern Brazilian Pleistocene mammals from Touro Passo Formation, and remarks on the geochronology, fauna and palaeoenvironments. Quaternary International 245 (2): 201-208. https://doi:10.1016/j.quaint.2010.10.010

Kramarz, A.G.; Bond, M. 2005. Los Litopterna (Mammalia) de la Formación Pinturas, Mioceno Temprano-Medio de Patagonia. Ameghiniana 42: 611-625.

Lobo, L.; Gelfo, J.N.; de Azevedo, S.A.K. 2024. The phylogeny of Macraucheniidae (Mammalia, Panperissodactyla, Litopterna) at the genus level. Journal of Systematic Palaeontology. https://doi.org/10.1080/14772019.2024.2364201

Marshall, L.G. 1976. Fossil localities for Santacrucian (Early Miocene) mammals, Santa Cruz Province, Southern Patagonia, Argentina. Journal of Paleontology 50: 1129-1142.

Marshall, L.G.; Salinas, P. 1990. Stratigraphy of the Río Frías Formation (Miocene), along the Alto Río Cisnes, Aisén, Chile. Revista Geológica de Chile 17 (1): 57-87.

Matheos, S.D.; Raigemborn, M.S. 2012. Sedimentology and paleoenvironment of the Santa Cruz Formation. *In* Early Miocene Paleobiology in Patagonia: high latitude paleocommunities of the Santa Cruz Formation (Vizcaíno, S.F.; Kay, R.F.; Bargo, M.S.; editors). Cambridge University Press: 59-82. Cambridge.

McGrath, A.J.; Anaya, F.; Croft D. A. 2018. Two new macraucheniids (Mammalia: Litopterna) from the late middle Miocene (Laventan South American Land Mammal Age) of Quebrada Honda, Bolivia. Journal of Vertebrate Paleontology: e1461632. https://doi.org/10.1080/02724634.2018.1461632

McGrath, A.J.; Flynn, J.J.; Wyss, A.R. 2020a. Proterotheriids and macraucheniids (Litopterna: Mammalia) from the Pampa Castillo Fauna, Chile (early Miocene, Santacrucian SALMA) and a new phylogeny of Proterotheriidae. Journal of Systematic Palaeontology 18 (9): 717-738. https://doi.org/10.1080/14772019.2019.1662500

McGrath, A.; Anaya, F.; Croft, D. 2020b. New Proterotheriids from the middle Miocene of Quebrada Honda, Bolivia, and body size and diversity trends in Proterotheriid and Macraucheniid Litopterns (Mammalia). Ameghiniana 57 (2): 159-188. https://doi.org/10.5710/amgh.03.03.2020.3268

McKenna, M.C.; Bell, S.K. 1997. Classification of Mammals Above the Species Level. Columbia University Press: 631 p. New York.

Monsalvo, E.S.; Costamagna, D. 2023. Estimación de la masa corporal de los Proterotheriidae (Mammalia, Litopterna). Publicación Electrónica de la Asociación Paleontológica Argentina 23 (R1): R160. https://doi:10.5710/PEAPA.23.03.2023.462

Muzzopappa, P.; Bargo, M.S.; Vizcaíno, S.F. 2025. Anurans from the early-middle Miocene Santa Cruz Formation at Río Chalía (Patagonia, Argentina), and a revision of the fossil Calyptocephalellidae (Anura, Australobatrachia). Journal of Systematic Paleontology 23 (1). https://doi.org/10.1080/14772019.2025.2456622

Pascual, R.; Ortiz-Jaureguizar, E.; Prado, J.L. 1996. Land mammals: paradigm for Cenozoic South American geobiotic evolution. *In* Contribution of Southern South America to Vertebrate Paleontology (Arratia, G.; editor). Munchner Geowissenshaftliche Abhandlungen: 265-319. Munich.

Patterson, B.; Pascual, R. 1968. The fossil mammal fauna of South America. The Quarterly Review of Biology 43 (4): 409-451.

Paula Couto, C. 1952. Fossil mammals from the beginning of the Cenozoic in Brazil: Condylarthra, Litopterna,

Xenungulata, and Astrapotheria. Bulletin of American Museum of Natural History 99: 355-394.

Püschel, H.P.; Alarcón-Muñoz, J.; Soto-Acuña, S.; Ugalde, R.; Shelley, S.L.; Brusatte, S.L. 2023. Anatomy and phylogeny of a new small macraucheniid (Mammalia: Litopterna) from the Bahía Inglesa Formation (late Miocene), Atacama Region, Northern Chile. Journal of Mammalian Evolution 30: 415-460. https://doi.org/10.1007/s10914-022-09646-0

Püschel, H.P.; Shelley, S.; Williamson, T.E.; Perini, F.A.;Wible, J.R.; Brusatte, S.L. 2024. A new dentition-based phylogeny of Litopterna (Mammalia: Placentalia) and 'archaic' South American ungulates, Zoological Journal of the Linnean Society 202 (1) https://doi.org/10.1093/zoolinnean/zlae095

Raigemborn, M.S.; Matheos, S.D.; Krapovickas, V.; Vizcaíno, S.F.; Bargo, M.S.; Kay, R.F.; Fernicola, J.C.; Zapata, L. 2015. Paleoenvironmental reconstruction of the coastal Monte León and Santa Cruz formations (Early Miocene) at Rincón del Buque, Southern Patagonia: A revisited locality. Journal of South American Earth Sciences 60: 31-55. https://doi.org/10.1016/j.jsames.2015.03.001

Raigemborn, M.S.; Krapovickas, V.; Zucol, A.F.; Zapata, L.; Beilinson, E.; Toledo, N.; Perry, J.; Lizzoli, S.; Martegani, L.; Tineo, D.; Passeggi, E. 2018. Paleosols and related soil-biota of the early Miocene Santa Cruz Formation (Austral-Magallanes Basin, Argentina): a multidisciplinary approach to reconstructing ancient terrestrial landscapes. Latin American Journal of Sedimentology and Basin Analysis 25 (2): 117-148.

Roth, S. 1899. Aviso preliminar sobre mamíferos mesozoicos encontrados en Patagonia. Revista del Museo de La Plata 9: 381-388.

Schmidt, G.I. 2015. Actualización sistemática y filogenia de los Proterotheriidae (Mammalia, Litopterna) del 'Mesopotamiense' (Mioceno tardío) de Entre Ríos, Argentina. Revista Brasileira de Paleontologia 18 (3): 521-546. https://doi: 10.4072/rbp.2015.3.14

Schmidt, G.I.; Ferrero, B.S. 2014. Taxonomic reinterpretation of *Theosodon hystatus* Cabrera and Kraglievich, 1931 (Litopterna, Macraucheniidae) and phylogenetic relationships of the family. Journal of Vertebrate Paleontology 34 (5): 1231-1238. https://doi.org/10.1080/02724634.2014.837393

Schmidt, G.I.; Hernández del Pino, S.; Muñoz, N.A.; Fernández, M. 2019. Litopterna (Mammalia) from the Santa Cruz Formation (Early-Middle Miocene) at the Río Santa Cruz, Southern Argentina. Publicación Electrónica de la Asociación Paleontológica Argentina 19 (2): 170-192. https://doi.org/10.5710/PEAPA.13.08.2019.290

Schmidt, G.I.; Armella, M.A.; Bonini, R.A. 2024. Updated record of Proterotheriidae (Litopterna, Mammalia) from the late Neogene of northwestern Argentina. Historical Biology 37 (5). https://doi.org/10.1080/08912963.2024.2359471

Scott, W.B. 1910. Mammalia of the Santa Cruz beds. Part I: Litopterna. Reports of the Princeton University Expedition to Patagonia. *In* Reports of the Princeton University Expedition to Patagonia (1896-1899) (Scott, W.B.; editor). Princeton University, E. Schweizerbart'sche Verlashandlung: 1-156. Stuttgart.

Simpson, G.G. 1980. Splendid Isolation: the curious history of South American mammals. Yale University Press: 266 p. New Haven.

Soria, M.F. 1981. Los Litopterna del Colhuehuapense (Oligoceno Tardío) de la Argentina. Revista del Museo Argentino de Ciencias Naturales "Bernardino Rivadavia", Serie Paleontología 3: 1-54.

Soria, M.F. 2001. Los Proterotheriidae (Mammalia, Litopterna): sistemática, origen y filogenia. Monografías del Museo Argentino de Ciencias Naturales "Bernardino Rivadavia" 1: 1-167.

Tauber, A.A. 1999. Los vertebrados de la Formación Santa Cruz (Mioceno inferior-medio) en el extremo sureste de la Patagonia y su significado paleoecológico. Revista Española de Paleontología 14: 173-182.

Trayler, R.B.; Schmitz, M.D.; Cuitiño, J.I.; Kohn, M.J.; Bargo, M.S.; Kay, R.F.; Stromberg, C.A.E.; Vizcaíno, S.F. 2020a. An improved approach to age-modeling in deep time: Implications for the Santa Cruz Formation, Argentina. Geological Society of America, Bulletin 132 (1-2): 233-244. https://doi.org/10.1130/B35203.1

Trayler, R.B.; Kohn, M.J.; Bargo, M.S.; Cuitiño, J.I.; Kay, R.F.; Strömbergn, C.A.E.; Vizcaíno, S.F. 2020b. Patagonian Aridification at the Onset of the mid-Miocene Climatic Optimum. Paleoceanography and Paleoclimatology 35 (9). https://doi.org/10.1029/2020PA003956

Ubilla, M.; Perea, D.; Bond, M.; Rinderknecht, A. 2011. The first cranial remains of the Pleistocene proterotheriid *Neolicaphrium* Frenguelli, 1921 (Mammalia, Litopterna): a comparative approach. Journal of Vertebrate Paleontology 31 (1): 193-201. https://doi.org/10.1080/02724634.2011.539647

Villafañe, A.L.; Ortiz-Jaureguizar, E.; Bond, M. 2006. Cambios en la riqueza taxonómica y en las tasas de primera y última aparición de los Proterotheriidae (Mammalia, Litopterna) durante el Cenozoico. Estudios Geológicos 62 (1): 155-166.

Villafañe, A.L.; Schmidt, G.I.; Cerdeño, E. 2012. Consideraciones sistemáticas y bioestratigráficas acerca de Thoatheriopsis mendocensis Soria, 2001

(Litopterna, Proterotheriidae). Ameghiniana 49 (3): 365-374. https://doi.org/10.5710/AMGH.v49i3(480)

Vezzosi, R.; Schmidt, G.I.; Brunetto, E. 2009. Un Proterotheriinae (Proterotheriidae: Litopterna) en el Pleistoceno tardío-Holoceno temprano (Lujanense) de Santa Fe. *In* Jornadas Argentinas de Paleontología de Vertebrados, No. 24. Ameghiniana 46 (4): 54R. San Rafael, Mendoza.

Vizcaíno, S.F.; Kay, R.F.; Bargo, M.S. 2012a. Early Miocene Paleobiology in Patagonia: High-latitude Paleocommunities of the Santa Cruz Formation. Cambridge University Press, Cambridge: 370 p.

Vizcaíno, S.F.; Kay, R.F.; Bargo, M.S. (Editors). 2012b. Background for a paleoecological study of the Santa Cruz Formation (late Early Miocene) on the Atlantic Coast of Patagonia. In Early Miocene Paleobiology in Patagonia: high-latitude paleocommunities of the Santa Cruz Formation. Cambridge University Press: 1-22. Cambridge. https://doi.org/10.1017/CBO9780511667381.002

Vizcaíno, S.F.; Bargo, M.S.; Cuitiño, J.I.; Pérez, M.E.; Muñoz, N.A.; Aramendía, I.; Tomassini, R.L.; Kay, R.F. 2018. The outstanding Río Chalía (= Sehuén) outcrops of the Santa Cruz Formation (Early Miocene, Burdigalian) and its fossil vertebrate content. Publicación Electrónica de la Asociación Paleontológica Argentina 19: 85R.

Vizcaíno, S.F.; Bargo, M.S.; Kay, R.F.; Raigemborn, M.S. 2021. The record of the typothere Pachyrukhos (Mammalia, Notoungulata) and the chinchillid Prolagostomus (Mammalia, Rodentia) in the Santa Cruz Formation (early-middle Miocene) south to the Río Coyle, Patagonia, Argentina. Publicación Electrónica de la Asociación Paleontológica Argentina 21 (2): 1-15.

Vizcaíno, S.; Bargo, M.S.; Pérez, M.; Aramendía, I.; Cuitiño, J.; Monsalvo, E.; Vlachos, E.; Noriega, J.; Kay, R. 2022. Fossil vertebrates of the early-middle Miocene Cerro Boleadoras Formation, northwestern Santa Cruz Province, Patagonia, Argentina. Andean Geology 49 (3): 382-422. https://dx.doi.org/10.5027/andgeoV49n3-3425

Welker, F.; Collins, M.J.; Thomas, J.A.; Wadsley, M.; Brace, S.; Cappellini, E.; Turvey, S.T.; Reguero, M.A.; Gelfo, J.N.; Kramarz, A.G.; Burger, J.; Thomas-Oates, J.; Ashford, D.A.; Ashton, P.D.; Rowsell, K.; Porter, D.M.; Kessler, B.; Fischer, R.; Baessmann, C.; Kaspar, S.; Olsen, J.V.; Kiley, P.; Elliott, J.A.; Kelstrup, C.D.; Mullin, V.; Hofreiter, M.; Willerslev, E.; Hublin, J.J.; Orlando, L.; Barnes, I.; MacPhee, R.D.E.; Hofreiter, M. 2015. Ancient proteins resolve the evolutionary history of Darwin's South American ungulates. Nature 522 (7554): 81-84. https://doi.org/10.1038/nature14249

Westbury, M.; Baleka, S.; Barlow, A.; Hartmann, S.; Paijmans, J.L.A.; Kramarz, A.; Forasiepi, A.M.; Bond, M.; Gelfo, J.N.; Reguero, M.A.; López-Mendoza, P.; Taglioretti, M.; Scaglia, F.; Rinderknecht, A.; Jones, W.; Mena, F.; Billet, G.; de Muizon, C.; Aguilar, J.L.; MacPhee, R.D.E.; Hofreiter, M. 2017. A mitogenomic timetree for Darwin's enigmatic South American mammal *Macrauchenia patachonica*. Nature Communications 8:15951. https://doi: 10.1038/ncomms15951

Manuscript received: October 18, 2024; revised/accepted: December 02, 2025; available online: December 11, 2025.

Appendix

List of specimens studied

List of specimens studied in this article, including their descriptions, as well as their geographical and altitudinal provenance. Additionally, comparative specimens from various national and foreign collections are provided.

Taxon	Specimen number	Referred material	Localities*	Altitudinal range (m a.s.l.)
Tetramerorhinus lucarius Ameghino, 1894	MPM-PV 21907	Right premaxillary fragment with a small incisor, left maxillary fragment with DP3-4, right mandibular fragment with dp1-4, and left mandibular fragment with broken dp4 and m1.	Río Chalía, P2 locality, Estancia Vivin Aike.	350-400
Tetramerorhinus cingulatum (Ameghino, 1891)	MPM-PV 21874	Right mandibular ramus with p4-m3 and left mandibular ramus with m1-m3.	Río Chalía, P7 locality, Estancia Las Horquetas.	150-250
Thoatherium minusculum Ameghino, 1887	MPM-PV 21877	Left maxillary fragment with roots of DP1-4 and M1.	Río Chalía, P2 locality, Estancia Vivin Aike.	150-250
Thoatherium minusculum	MPM-PV 21903	Right dp2.	Río Chalía, P8 locality, Estancia Las Horquetas.	150-250
Thoatherium minusculum	MPM-PV 21900	Incomplete left dp3 and dp4.	Río Chalía, P3 locality, Estancia Vivin Aike.	150-250
Thoatherium minusculum	MPM-PV 21937	Skull portion associated with a left mandibular fragment with p3 (isolated)-m3 and a right one with p4-m3.	Río Chalía, P6 locality, Estancia Los Sauces.	150-250
Thoatherium minusculum	MPM-PV 21899	Isolated teeth. Right: M1, M3, p4?, and m3. Left: M1-M3, and m2-3	Río Chalía, P2 locality, Estancia Vivin Aike.	350-400
Diadiaphorus majusculus Ameghino, 1887	MPM-PV 21881	Right maxillary fragment with incomplete P3-P4.	Río Chalía, P8 locality, Estancia Las Horquetas.	150-250
Diadiaphorus majusculus	MPM-PV 21882	Left P3 and M2 (incomplete), and right M1 and M3.	Río Chalía, P8 locality, Estancia Las Horquetas.	150-250
Diadiaphorus majusculus	MPM-PV 21884	Left maxillary fragment with posterior root of P2 and P3 without labial side.	Río Chalía, P8 locality, Estancia Las Horquetas.	150-250
Diadiaphorus majusculus	MPM-PV 21902	Left mandibular fragment with p3 (broken) and p4.	Río Chalía, P8 locality, Estancia Las Horquetas.	150-250
Diadiaphorus majusculus	MPM-PV 22340	Incomplete right m3.	Río Chalía, P7 locality, Estancia Las Horquetas.	150-250
Anisolophus australis (Burmeister, 1879)	MPM-PV 21898	Upper incisor and left mandibular fragment with p4.	Río Chalía, P2 locality, Estancia Vivin Aike.	350-400
Anisolophus australis	MPM-PV 21879	Right mandibular fragment with broken p4, m1-2, and erupting m3.	Río Chalía, P2 locality, Estancia Vivin Aike.	250-350

List of specimens studied continued.

Taxon	Specimen number	Referred material	Localities*	Altitudinal range (m a.s.l.)
Anisolophus australis	MPM-PV 21878	Isolated p2, left mandibular fragment with p4-m1, and an isolated m3 with its labial side broken.	Río Chalía, P2 locality, Estancia Vivin Aike.	250-350
Anisolophus floweri Ameghino, 1887	MPM-PV 21880	Broken left M2.	Río Chalía, P8 locality, Estancia Las Horquetas.	150-250
Anisolophus floweri	MPM-PV 21905	Right m2.	Río Chalía, P6 locality, Estancia Los Sauces.	250-350
Anisolophus floweri	MPM-PV 21901	Lingual side of right m3.	Río Chalía, P7 locality, Estancia Las Horquetas.	150-250
Theosodon sp.	MPM-PV 21876	Left P3.	Río Chalía, P2 locality, Estancia Vivin Aike.	350-400
Theosodon sp.	MPM-PV 21883	Left mandibular fragment with dp3.	Río Chalía, P8 locality, Estancia Las Horquetas.	150-250
Theosodon sp.	MPM-PV 21875	Left calcaneus.	Río Chalía, P7 locality, Estancia Las Horquetas.	250-300

*All localities in the Corpen Aike Department, Province of Santa Cruz, Argentina.

Comparative Material

Taxon	Specimen Number	Geographical Provenance
Thoatherium minusculum Ameghino, 1887	FMNH P 13193	Río Coyle, Santa Cruz
	YPM VPPU 15236	Río Coyle, Santa Cruz
	MACN-A 1855	Karaiken, Santa Cruz
	MACN-A 3000	Corriguen-Kaik, Santa Cruz
	MACN-A 3002-03	Corriguen-Kaik, Santa Cruz
	MACN-A 9080-81	Corriguen-Kaik, Santa Cruz
	MACN-A 9082	Monte Observación, Santa Cruz
	MPM-PV 3682	Puesto Estancia La Costa*, Santa Cruz
	MPM-PV 19150	Cerro Boleadoras, Santa Cruz
	MPM-PV 19453	Río Santa Cruz, Santa Cruz
	MPM-PV 19457	Río Santa Cruz, Santa Cruz
	MPM-PV 19458	Río Santa Cruz, Santa Cruz
	MPM-PV 19459	Río Santa Cruz, Santa Cruz
	MPM-PV 19460	Río Santa Cruz, Santa Cruz

Comparative material continued.

Taxon	Specimen Number	Geographical Provenance
Tetramerorhinus lucarius Ameghino, 1894	MACN-A 3021 (Type)	Monte Observación, Santa Cruz
	MACN-A 1843-44	Karaiken, Santa Cruz
	MPM-PV 3529	Puesto Estancia La Costa*, Santa Cruz
	MACN-A 3020	Monte Observación, Santa Cruz
	MACN-A 190	Santa Cruz
Tetramerorhinus cingulatum (Ameghino, 1891)	MACN-A 3065-66 (Type)	Sehuen, Santa Cruz
	MACN-A 8665	Corriguen-Kaik, Santa Cruz
	MACN-A 3062	Sehuen, Santa Cruz (?)
Diadiaphorus majusculus Ameghino, 1887	MLP-PV 12-333 (Type)	Río Santa Cruz, Santa Cruz
	MLP-PV 12-325	Monte León, Santa Cruz
	AMNH 9270	Monte Casa, Santa Cruz
	MACN-A 9198-99	Corriguen-Kaik, Santa Cruz
	MACN-A 9200-08	Corriguen Aike, Santa Cruz
	MLP-PV 12-253	Santa Cruz
	MLP-PV 12-254	Santa Cruz
	MLP-PV 12-305	Santa Cruz
Anisolophus australis (Burmeister, 1879)	MACN-PV 2417 (Type)	Rio Chico, Santa Cruz
	MACN-A 1861	Santa Cruz
	MACN-A 3107	Monte Observación, Santa Cruz
	MLP-PV 12-336	Santa Cruz
	MLP-PV 12-341	Santa Cruz
Anisolophus floweri (Ameghino, 1887)	MPM-PV 19429	Río Santa Cruz, Santa Cruz
	MACN-A 9003-12	Yegua Quemada, Santa Cruz
	MACN-A 3098	Monte Observación, Santa Cruz
	YPM-VPPU 15309	Río Coyle, Santa Cruz
	MLP-PV 12-289	Santa Cruz
	MPM-PV 19432	Río Santa Cruz, Santa Cruz
	MPM-PV 19442	Río Santa Cruz, Santa Cruz
Theosodon fontanae Ameghino, 1891	MACN-A 2701 (Type)	Sehuen, Santa Cruz
Theosodon garrettorum Scott, 1910	YPM-VPPU 15164	Güer Aike, Santa Cruz
Theosodon lydekkeri Ameghino, 1887	MACN-A 9269-88	Corriguen Aike, Santa Cruz
Theosodon cf. *lydekkeri*	MPM-PV 17481	Anfiteatro, Santa Cruz
Theosodon sp.	MACN-PV 17625	Río Santa Cruz, Santa Cruz
"*Theosodon arozquetai*" McGrath, Anaya and Croft, 2018	UATF-V-001940	Quebrada Honda, Bolivia
Cramauchenia normalis Ameghino, 1902	MPEF-PV 2524	Cabeza Blanca, Chubut
Theosodon lallemanti Mercerat, 1891	YPM-VPPU 016002	Santa Cruz

*Puesto Estancia La Costa (= Corriguen Aike, Corriken Aike, Corriguen Kaik; Vizcaíno *et al*., 2012b). All the listed taxa are Santacrucian in age.